

<b>REPORT DOCUMENTATION PAGE</b>			Form Approved OMB No. 0704-0188	
Public reporting burden for this collection of information is estimated to average 1 hour per response, including the time for reviewing instructions, searching existing data sources, gathering and maintaining the data needed, and completing and reviewing the collection of information. Send comments regarding this burden estimate or any other aspect of this collection of information, including suggestions for reducing this burden, to Washington Headquarters Services, Directorate for Information Operations and Reports, 1215 Jefferson Davis Highway, Suite 1204, Arlington, VA 22202-4302, and the Office of Management and Budget, Paperwork Reduction Project (0704-0188), Washington, DC 20503.				
1. AGENCY USE ONLY (Leave Blank)	2. REPORT DATE 12/06/01	3. REPORT TYPE AND DATES COVERED May 10, 2001 - November 10, 2001		
4. TITLE AND SUBTITLE High Energy Metallic Mechanical Alloys for New Explosives and Incendiary Devices with Controllable Explosion Parameters			5. FUNDING NUMBERS DTRA 01-01-P-0158	
6. AUTHOR(S) Dr. Emil Shtessel Dr. Edward Dreizin				
7. PERFORMING ORGANIZATION NAME(S) AND ADDRESS(ES) Exotherm Corporation, 1035 Line Street, Camden, NJ 08103  New Jersey Institute of Technology, Newark, NJ 07102-1982			8. PERFORMING ORGANIZATION REPORT NUMBER Exotherm-NJIT-TR-01	
9. SPONSORING/MONITORING AGENCY NAME(S) AND ADDRESS(ES) Defense Threat Reduction Agency 6801 Telegraph Road Alexandria, VA 22310			10. SPONSORING/MONITORING AGENCY REPORT NUMBER	
11. SUPPLEMENTARY NOTES				
12a. DISTRIBUTION/AVAILABILITY STATEMENT (see Section 5.3b of this solicitation)  Approved for public release			12b. DISTRIBUTION CODE	
13. ABSTRACT (Maximum 200 words) Report developed under SBIR contract for topic DTRA 01-011. The feasibility of production of metastable mechanical alloys is demonstrated and combustion behavior of alloys and pure metals is compared. Sets of Al-Mg, Al-Mg-H, B-Mg, Al-B, and Ti-B mechanical alloys were prepared. X-ray diffraction, electron microscopy, and laser diffraction were used to characterize structures, morphology, and sizes of the produced alloys, respectively. The produced materials were nano-crystalline metastable phases with particle sizes in the range of 1 - 50 µm. A constant volume explosion technique was used to evaluate performance of the produced alloys and to compare it to that of pure metal powders of different sizes and morphologies. The recorded pressure traces served as the main piece of experimental information, combustion products were also collected and analyzed. The results have clearly shown that the combustion behavior of pure boron and aluminum powders can be dramatically improved by alloying these materials with Ti and Mg, respectively. Preliminary results also indicate improved boron combustion when boron is alloyed with Mg. Alloying boron with Al showed no such improvement, however. The improvements in the ignition and combustion parameters are found to be significant even though quite coarse mechanical alloy powders were prepared and tested in this effort. The relatively large size of mechanical alloy powders is expected to be advantageous in practical applications requiring mixing and handling of the energetic metal powders.				
14. SUBJECT TERMS SBIR report metals alloys energetic aluminum boron magnesium titanium			15. NUMBER OF PAGES 36	
			16. PRICE CODE	
17. SECURITY CLASSIFICATION OF REPORT Unclassified	18. SECURITY CLASSIFICATION OF THIS PAGE Unclassified	19. SECURITY CLASSIFICATION OF ABSTRACT Unclassified	20. LIMITATION OF ABSTRACT UL	

REF E

20011211 156

**HIGH ENERGY DENSITY METALLIC MECHANICAL ALLOYS FOR NEW  
EXPLOSIVES AND INCENDIARY DEVICES WITH CONTROLLABLE  
EXPLOSION PARAMETERS**

**SBIR Phase I Final Report**

Contract Number: DTRA 01-01-p-0158

**Prepared for:** Dr. Kibong Kim, DTRA  
Defense Threat Reduction Agency  
6801 Telegraph Road  
Alexandria, VA 22310

**Prepared by:** Dr. Emil Shtessel  
EXOTHERM Corporation  
1035 Line Street  
Camden, NJ 08103

and

Dr. Edward Dreizin<sup>1</sup>  
New Jersey Institute of Technology  
Department of Mechanical Engineering  
University Heights  
Newark, NJ 07102-1982

December 6, 2001

---

<sup>1</sup> The research at NJIT was jointly supported by subcontract from Exotherm Corporation and by the US Office of Naval Research, Award N000140010446 (Technical Monitor Dr. Judah Goldwasser)

<b>I. INTRODUCTION</b>	<b>3</b>
<b>A. Summary of Phase I Results</b>	<b>3</b>
<b>B. Background</b>	<b>3</b>
<b>II. PHASE I TECHNICAL OBJECTIVES</b>	<b>5</b>
<b>III. MECHANICAL ALLOY PREPARATION TECHNIQUE</b>	<b>5</b>
<b>IV. MATERIALS CHARACTERIZATION TECHNIQUES</b>	<b>6</b>
<b>V. MATERIALS</b>	<b>7</b>
<b>A. Pure metals</b>	<b>7</b>
<b>B. Raw Materials for Mechanical Alloys</b>	<b>9</b>
<b>C. Mechanical alloys</b>	<b>9</b>
Al-Mg system	9
Al-Mg-H system	13
B-Ti system	16
Al-B and Mg-B systems	20
<b>VI. EXPLOSION APPARATUS AND TECHNIQUES</b>	<b>21</b>
<b>A. Apparatus</b>	<b>21</b>
<b>B. Techniques</b>	<b>22</b>
<b>VII. EXPLOSION EXPERIMENTS RESULTS AND DISCUSSION</b>	<b>23</b>
<b>A. Mg-Al and Al-Mg-H Systems</b>	<b>24</b>
<b>B. B-Mg and B-Al Systems</b>	<b>30</b>
<b>C. B-Ti Systems</b>	<b>30</b>
<b>D. Aluminum powders with different size distributions</b>	<b>33</b>
<b>VIII. CONCLUSIONS</b>	<b>34</b>

## **I. INTRODUCTION**

### **A. Summary of Phase I Results**

This research addressed the feasibility of the production of a wide range of metastable mechanical alloys and demonstrating their improved combustion behavior as compared to the pure metals. High-energy ball milling was used to prepare sets of Al-Mg, Al-Mg-H, B-Mg, Al-B, and Ti-B mechanical alloys. X-ray diffraction, electron microscopy, and low angle laser diffraction techniques were used to characterize structures, morphology, and sizes of the produced alloys, respectively. The produced materials were nano-crystalline metastable phases with particle sizes in the range of 1 – 50  $\mu\text{m}$ .

A constant volume explosion technique was used to evaluate performance of the produced novel mechanical alloys and to compare it to that of pure metal powders of different sizes and morphologies. The pressure traces recorded in real time served as the main piece of experimental information. After selected experiments, combustion products were collected and analyzed.

The results of this effort have clearly shown that the combustion behavior of pure boron and aluminum powders can be dramatically improved by alloying these materials with Ti and Mg, respectively. Preliminary results also indicate improved boron combustion when boron is alloyed with Mg. Alloying boron with Al showed no such improvement, however.

The improvements in the ignition and combustion parameters are found to be significant even though quite coarse mechanical alloy powders were prepared and tested in this effort. The relatively large size of mechanical alloy powders is expected to be advantageous in many practical applications requiring mixing and handling of the energetic metal powders.

### **B. Background**

Properties of explosives used in different weapons could be tailored to defeat specific targets, including a variety of underground facilities if the blast pressure and the rate of the produced heat release are readily controlled. Presently, the means of such control are quite limited and in most cases require changes in the total mass of the explosive charge. Metal additives, e.g., aluminum powders are routinely added to explosives to increase heat release and produce a longer duration pressure pulse. However, it is widely recognized that the benefits expected from metal additives are not fully achieved, mostly due to the long ignition delays and slow combustion rates of metals. In addition, the decrease in the detonation velocity caused by metal additives significantly limits the capability of producing sharp pressure pulses required for many applications. Currently, an opportunity of varying the metal particle sizes, especially using nano-sized metal powders in explosive formulations, is being explored as a means to achieve faster ignition and higher rates of heat release. While some promising results have been reported, several important limitations of this approach have also emerged. Among the most significant problems is the high sensitivity of nano-sized powders resulting in the deterioration of their properties in relatively short time periods and making handling of

these powders difficult. Another drawback is the poor repeatability of the powder parameters and performance caused by seemingly insignificant variations in their preparation technology. The preparation of various size batches of particles with narrow size distributions is difficult and expensive, and, finally, change of particle size may not be sufficient to achieve the desired degree of blast control. Therefore, the metal particle size may not be the only parameter suitable to control the blast parameters desired for new weapons systems, and some alternative approaches need to be investigated.

Recently, research of the mechanisms of metal combustion [1 - 8] has shown that both ignition delay and combustion rate are strongly affected by phase changes occurring in the burning metals. Based on these results, *new types of metal-based high energy density materials have been proposed in which specific phase changes are predetermined to occur at a desired temperature and either trigger ignition or increase combustion rate of the metallic fuel.* Because the desired phase change should occur rapidly, the new metal-based energetic compounds should be metastable, e.g., supersaturated solid solutions that include a base metal as a solvent and another component (that could be a metal or gas, such as hydrogen) as a solute. Such metastable Al-Mg solid solutions have recently been prepared in laboratory quantities (tens of grams) using a novel technique of mechanical alloying (MA) [9]. MA is a relatively young material processing technique originally developed by Benjamin [10] and actively exploited in materials research and technology. Recent research in the area of new structural materials has shown that MA can be used, similar to rapid quenching, to produce highly metastable phases and supersaturated solid solutions [10 - 15]. It is a dry, high-energy ball milling process in which an initial blend of powders is repeatedly kneaded together and re-fractured by the action of the ball-powder collisions. The process usually produces a powder in which each particle has a composition similar to the bulk composition of the original powder blend. The mechanisms of MA include repeated cold welding and fracturing leading to ultra fine mixing and true alloying [10, 11]. While detailed understanding of MA is only being developed, the process finds numerous applications in metallurgy and materials processing because of its relative simplicity and efficiency [11]. MA has not been used to prepare high energy density materials until recent work [9] where Al-Mg mechanical alloys with Mg contents varying from 10 to 50 % have been prepared and tested. The average size of the produced Al-Mg particles was in the range of 5 - 15  $\mu\text{m}$  and depended on the alloy composition and milling parameters, but did not depend on the size of the precursor metal particles. Characterization of the MA powders showed that the aluminum crystal structure was generally preserved but the crystal lattice size increased to accommodate the solute atoms. The crystallite size decreased from 0.1  $\mu\text{m}$  (for the original Al powder) to 6 nm. Preliminary performances tests have indeed shown dramatically reduced ignition temperatures (e.g., 1150 K for a Al-10%Mg mechanical alloy versus 2200 K for the pure Al) and higher burn rates. Most importantly, preliminary observations have shown that the rate of heat release in combustion of the mechanically alloyed particles is much different from that of pure aluminum. It has been observed that the bulk of combustion heat for the MA particles is being released immediately at the ignition followed by slower heterogeneous particle combustion. In contrast, for aluminum, a longer ignition delay is followed by a relatively slow combustion period that is in turn followed by a more active heat release starting after about half of the total particle burn time. In summary, it has been shown that various

combustion rates and ignition temperatures can be achieved by controlling the composition of the Al-Mg mechanically alloyed powders.

*An opportunity identified in this proposed research is to explore the feasibility of using the new mechanically alloyed metallic powders with varied compositions and crystallite sizes as additives to explosive formulations that would enable one to control blast parameters in a wide range.* If successful, such materials can be used in a variety of explosive and incendiary devices and enable one to precisely adjust the produced blast parameters to defeat specific targets. In addition, admixtures of trace amounts of easily detectable elements could be added to mechanical alloys, such elements released in a blast would produce readily observable signatures required for damage assessment.

## **II. PHASE I TECHNICAL OBJECTIVES**

The following is a copy of the Phase I technical objectives proposed:

The overall objective of this proposed research is to develop a mechanical alloying technique for production of new, metallic, high energy density materials with controlled reaction parameters. Such materials will be used in the future explosive and incendiary devices to improve and, most importantly, control the produced blast characteristics, such as pressure trace, energy release rate, and optical radiation.

The objective of this Phase I effort is to demonstrate the feasibility of wide range control of the combustion and explosion parameters by adjusting the composition, structure, and crystallite size of mechanical alloys.

Specific objectives of the proposed project are:

1. Demonstrate that the ignition delay can be varied in a wide range by adjusting the mechanical alloy compositions and structure.
2. Demonstrate that choosing specific alloy compositions and crystallite sizes gives control over the pressure pulse produced by a mechanical alloy fuel-air explosion.
3. Demonstrate that the combustion of mechanical alloy powders can occur in a significantly leaner oxidizing environment as compared to similar pure metal powder combustion
4. Demonstrate that the properties of the mechanical alloys can remain stable over extended time periods and thus enable one to produce reliable weapon systems utilizing these materials.

## **III. MECHANICAL ALLOY PREPARATION TECHNIQUE**

Mechanical alloying was used for the preparation of metastable metal-based phases for combustion applications. A high-energy ball mill SPEX 8000, used in many experimental studies of MA, was also used for preparation of energetic mechanical alloys in this work. A zirconia vial and balls have been used to provide a chemically clean environment during ball milling of aluminum-based compounds (Al-Mg alloys). A stainless steel vial and balls were used to prepare boron-based compounds (Al-B, Ti-B,

and Mg-B alloys). The ball to powder mass ratio used in this project was 5; this parameter is known to affect the required time of milling. Balls of about 10 mm diameter were used, the diameter of balls is important for the overall milling time and also, for the final powder particle size distribution.

Process control agents (PCA) are frequently required in mechanical alloying to avoid domination of cold welding and formation of large agglomerates. Small amounts of PCA (on the level of 1-5 mass %) are usually added to the powder blend. Different PCA are used, some of the popular ones are stearic acid, hexane, and methanol. Stearic acid has been used in this project, and 2 mass % of PCA were added to the initial powder blend of all materials. Samples of B-Ti alloys were also prepared with no PCA added.

The mass of a single batch of the prepared mechanical alloy was 10 g and was limited in this project by the dimensions of the standard SPEX vials and safety considerations. The sample vial was filled with argon prior to the ball milling; it was opened in argon environment and slowly vented with air after the material was prepared. This treatment was observed to passivate some of the powders (e.g., B-Ti alloys) that were pyrophoric as prepared. The powder was dried in a vacuum chamber at room temperature to remove excess of the PCA material.

Preliminary experiments were conducted to determine the minimum time of ball milling necessary to achieve the "final" product structure, e.g., the maximum solubility of Mg in Al, etc. These experiments served to determine the final milling times for each materials system shown in Table 1.

Table 1. Milling times used to prepare mechanical alloys with a SPEX 8000 Ball mill

Material composition	Milling time, hours
Al-Mg	12
Al-Mg-H	21
Al-B	12
B-Mg	12
B-Ti	3

#### IV. MATERIALS CHARACTERIZATION TECHNIQUES

Phases of the produced powders were analyzed using x-ray diffraction (a Philips X'pert MRD x-ray diffractometer system). An Electro Scan environmental scanning electron microscope (SEM) integrated with Kevex Sigma 3 Energy Dispersive X-ray Spectroscopy detector (EDS) was used to study the morphology of the particles and their spatially resolved elemental compositions.

A commercial Coulter LS 230 Enhanced Laser Diffraction particle size analyzer was used to determine the particle size distribution for produced alloys as well as for their combustion products. The operation principle of the instrument uses low angle laser light scattering and the instrument is capable of working with particles from 0.04 to 2000  $\mu\text{m}$  diameter. A suspension of particles in a fluid is prepared and used for size distribution measurements with a "Small Volume Plus" unit. This technique provides a higher accuracy, works better with smaller size particle fractions, and is more time efficient than the microscopy-based image analysis. Distilled water served as a fluid for suspending the

powders of pure metals and Al-Mg alloys. Powder suspensions of Al-Mg-H and B-Ti mechanical alloys and products of the Al-Mg combustion were prepared using ethylene glycole as a fluid because these powders were found to react with water.

## V. MATERIALS

### A. Pure metals

Experiments were conducted with several samples of pure metal powders with different particle sizes. We used the following ultrafine aluminum powders supplied by Technanogy. Powder characterization as given by the manufacturer is shown below:

Materials Powder	TGA Quantity (g) % gain	BET Result M2/g	Particle Data				
			volume Result (ox/met)	ratio (nm)	oxide dia. thick. (nm) metal		wt% Al
B071301B	18	55.1	52.6	0.4171	37.1	2.0	62.0
B080701	10	62.4	48.5	0.2887	41.5	1.7	70.2
B091101A2	10	74.5	13.6	0.1314	154.9	3.1	83.8

Electron microscopy revealed that the particle sizes in the powders supplied by Technanogy varied significantly. Many large particles or dense agglomerates of small particles were observed as illustrated in Fig. 1, which was expected to affect the combustion behavior of these materials.



Fig. 1. Morphology of a B091101A2 powder sample by Technanogy (an SEM image). Very fine nano-sized particles are not resolved and seen as "fluff" surrounding large particles.

Size classified samples of pure aluminum powders were prepared using US standard sieves No 450 (nominal opening 32  $\mu\text{m}$ ) and No 635 (nominal opening 20  $\mu\text{m}$ ) and 98% pure spherical aluminum powders by Alpha Aesar and 99+ % pure, - 325 Mesh

(particles less than 44  $\mu\text{m}$ ) magnesium powder by Sigma Aldrich. The size distributions of the classified aluminum powders determined using the Coulter LS 230 analyzer are shown in Fig. 2. The morphology of the used spherical aluminum powders is illustrated in Fig. 3.

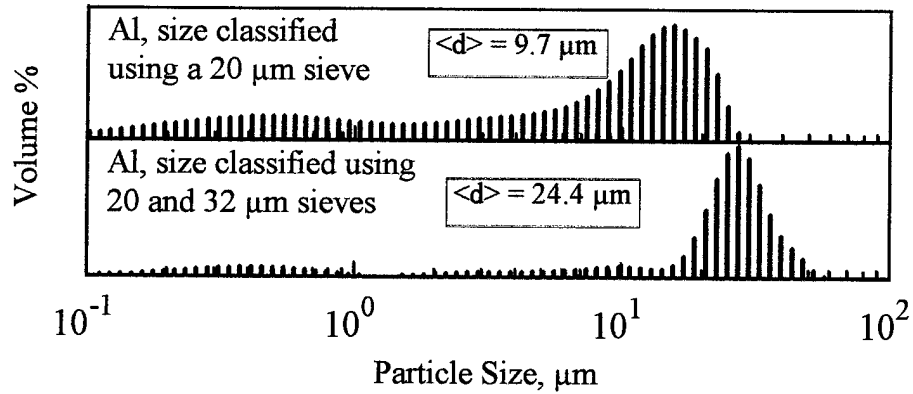


Fig. 2. Size distributions of the size classified, spherical, pure aluminum powders used for explosion tests. Mean particle sizes are labeled as  $\langle d \rangle$ .

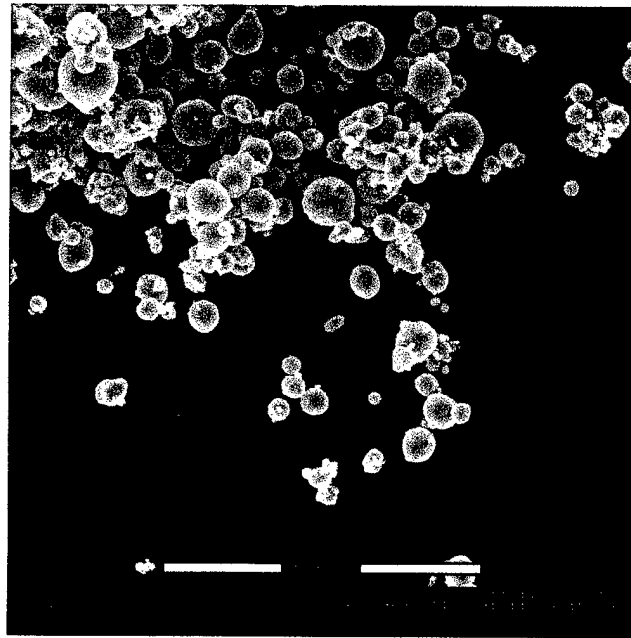


Fig. 3. Morphology of 98% pure spherical aluminum powders by Alpha Aesar (an SEM image).

Finally, -325 Mesh, 99.8% pure aluminum powder by Atlantic Equipment Engineers, -325 Mesh 99.9% pure magnesium powders by Aldrich Chemical, - 325mesh, 99.7% pure titanium powder by Atlantic Equipment Engineers, and 98.5% pure amorphous boron powder were used to prepare mechanical powder blends for comparison of their explosion parameters with mechanical alloys of identical composition.

## B. Raw Materials for Mechanical Alloys

The powders used for preparation of mechanical alloys were:

- Aluminum: 99.8 % pure, - 100 Mesh (particles less than 149  $\mu\text{m}$ ) by Atlantic Equipment Engineers
- Magnesium: 99+ % pure, - 50 Mesh (particles less than 297  $\mu\text{m}$ ) by Sigma Aldrich
- Magnesium Hydride (Assay),  $\text{MgH}_2$ , 90% pure (remainder Mg), by Aldrich Chemical Company
- Titanium: 99.7% pure; -325 Mesh by Atlantic Equipment Engineers (AEE)
- Boron: amorphous, 98.5 % pure; particle size less than 1  $\mu\text{m}$ , by AEE

## C. Mechanical alloys

### Al-Mg system

#### *Crystal Structure*

X-ray diffraction patterns showing the crystal structure evolution at different magnesium contents for the Al-Mg mechanical alloys are shown in Fig. 4. The initial Al-Mg powder blend clearly shows sets of both Al and Mg peaks. However, the Mg peaks completely disappear from the alloy diffraction patterns. The peaks of Al shift indicating an increase in the lattice parameter due to the dissolution of Mg in the structure. Using the experimental peak positions, the lattice parameter was found to increase from 4.05 Å for pure Al to 4.20 Å for the Al – 50 % Mg alloy. In addition, the width of the Al peaks increases implying a significant decrease in crystallite size. Our estimates using the Scherrer equation showed that the crystallite size decreased from about 0.1  $\mu\text{m}$  for aluminum to about 6 nm for the alloyed powders. While the equilibrium room temperature solubility of Mg in Al does not exceed 1 % [16], up to 30 % of Mg have been observed to dissolve in the prepared Al-Mg mechanical alloys. Therefore, the produced materials can be described as metastable, nano-phase solid solutions of Mg in Al. The x-ray analyses also showed that when the Mg contents exceed 30 %, an intermetallic phase  $\text{Al}_{12}\text{Mg}_{17}$  starts to form in the produced material.

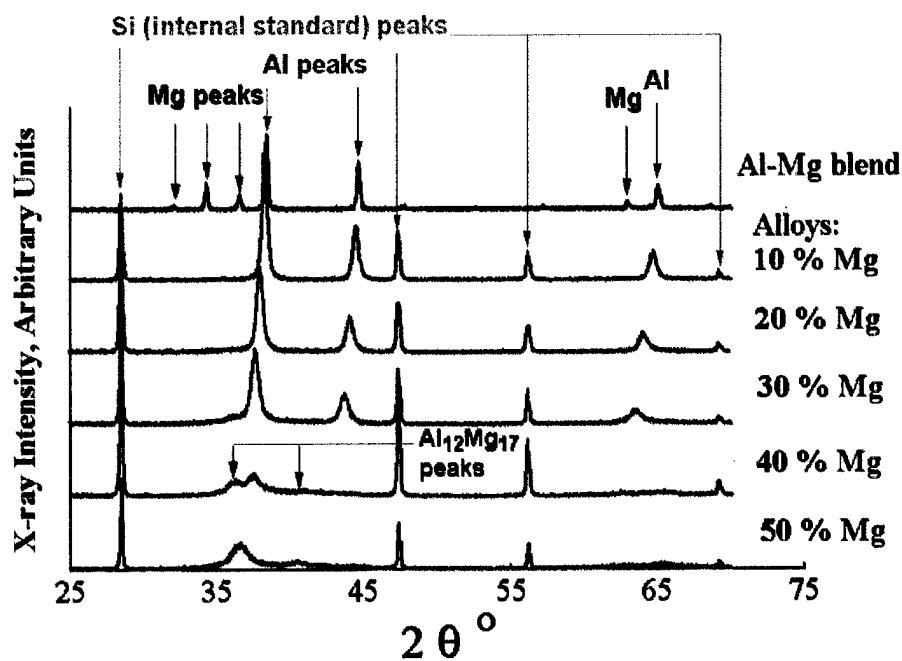


Fig. 4. X-ray patterns of the Al-Mg powder blend, and Al-Mg mechanical alloys

The approach of this study is based on the assumption that the metastable nature of the produced materials accounts for their accelerated ignition and combustion rate. Direct comparison of the combustion characteristics of the metastable mechanical alloys versus thermodynamically stable assemblages of the same bulk composition is needed to validate this approach. In order to provide such a validation, materials with the same bulk composition, particle morphologies, and most importantly, size distribution should be prepared to meaningfully compare their combustion characteristics. For simplicity, we annealed the metastable mechanically alloyed material at temperatures high enough to allow back-transformation to a thermodynamically stable state, but low enough to prevent significant alteration of particle size or agglomeration. The temperature where spontaneous back-transformation occurs was estimated by Differential Scanning Calorimetry (DSC). A sample of an  $\text{Al}_{0.7}\text{Mg}_{0.3}$  mechanical alloy was heated in a TA Instruments DSC 2920 at 10 K/min under a 50 ml/min flow of nitrogen. The exothermic back-transformation was observed to begin at 238 °C with a peak temperature of 253 °C. XRD analyses before and after the transition showed that the mechanical alloy has transformed to the intermetallic phase  $\text{Al}_2\text{Mg}_3$  and aluminum with a lesser amount of dissolved magnesium, as illustrated in Fig. 5. The enthalpy of the back-transformation was estimated to be 180 J/mol, or more than 3 orders of magnitude less than the metal oxidation enthalpy (e.g. 838 kJ per mole of aluminum for the formation of  $\text{Al}_2\text{O}_3$ ).

For a series of explosion tests batches of all the prepared Al-Mg mechanical alloys with magnesium content varied from 10 to 50 % were annealed in a furnace under vacuum at about 380 °C.

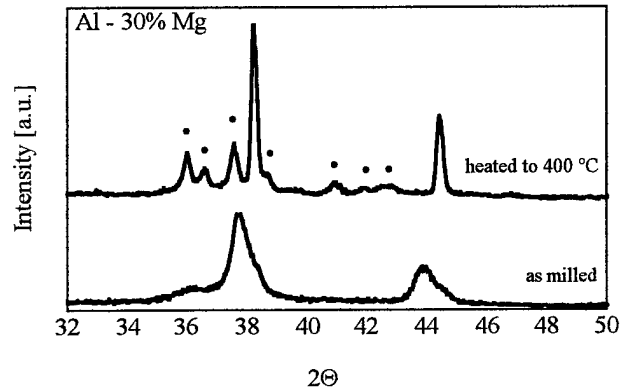


Fig. 5. XRD patterns of Al – 30% Mg mechanical alloy before and after annealing to 400 °C in a differential scanning calorimeter. Aluminum peaks have shifted back to their equilibrium positions (cf. Fig. 4). The marked peaks correspond to the stoichiometric phase  $\text{Al}_3\text{Mg}_2$ .

#### *Particle Sizes*

Particle size measurements summarized in Fig. 6 show little variation in the Al-Mg mechanical alloy particle sizes as a function of magnesium content. The measurements show that mechanical alloy powders have fairly wide size distributions with the mean particle sizes generally larger than for the pure magnesium and aluminum powders used in the reference powder blends. Note that the size of the mechanically alloyed powders can be controlled by the size of the balls used during the milling and by the type and amount of the process control agent [17], however, due to the limited time and scope of the present effort no such adjustments have been made.

#### *Particle Morphology*

Representative examples of the SEM images of different Al-Mg alloy particles are shown in Fig. 7. The shapes of the alloy particles were irregular, and it could be seen that the particles consisted of several layers. Some of the larger particles appeared as a group of smaller parts lumped together, however, we have not observed loose particle agglomerates. Therefore, it was expected that during dispersion, ignition, and combustion the densely agglomerated particles would behave as monolithic single particles. Based on both electron microscopy observations and particle size analysis results it could also be concluded that the Al-Mg alloys contained only a very small number of ultra fine particles. The surface morphology of particles was somewhat different for alloys with different elemental compositions. The edges of the particles of the alloy with 10 % of magnesium appeared more rounded than those of the alloys with higher magnesium contents. This shape difference is probably indicative of the increased alloy hardness for higher magnesium contents.

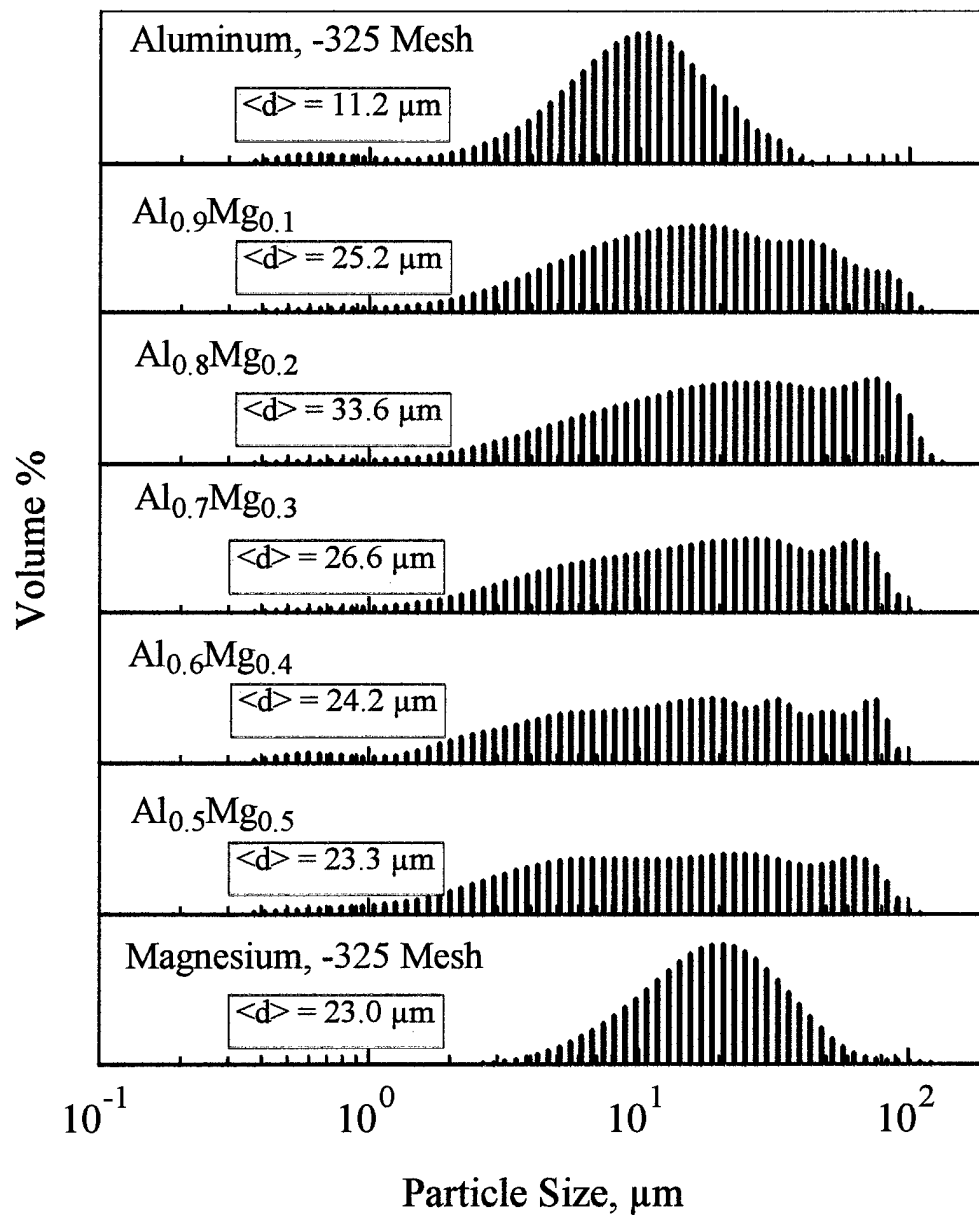


Fig. 6. Size distributions of the produced Al-Mg mechanical alloy powders and aluminum and magnesium powders used to prepare reference powder blends. Mean particle sizes are labeled as  $\langle d \rangle$ .

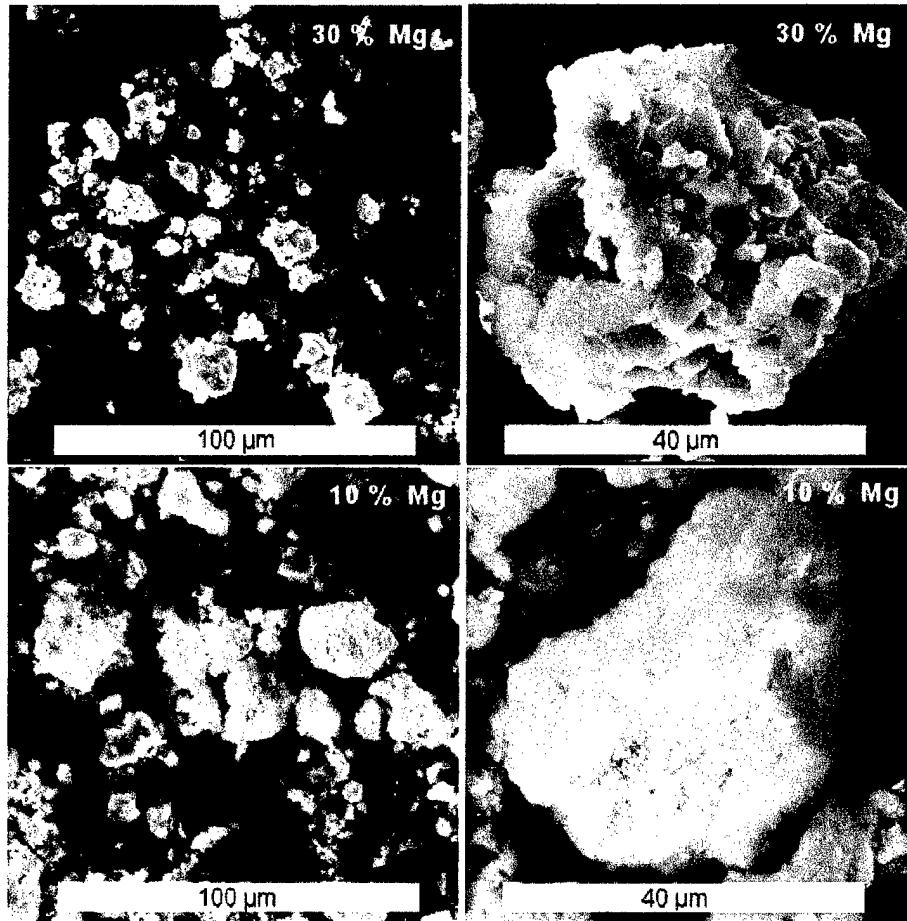


Fig. 7. SEM images of produced Al-Mg mechanical alloy powders

### Al-Mg-H system

#### *Crystal Structure*

The results of the x-ray diffraction measurements conducted for the prepared Al-Mg-H mechanical alloys (or Al-MgH<sub>2</sub> alloys) are shown in Fig. 8. The MgH<sub>2</sub> peaks are clearly observed in the initial powder blend and their intensities are significantly lower after ball milling, although they do not disappear completely from the x-ray patterns. This indicates incomplete dissolution of MgH<sub>2</sub> in aluminum. Peak widths for both Al and MgH<sub>2</sub> increase, indicating decreasing crystallite sizes. However, the shifts in the positions of the aluminum lattice peaks are barely noticeable in contrast to the quite substantial peak shifts observed for the Al-Mg mechanical alloys. The small shifts in the peak positions indicate that only minor adjustments occurred in the lattice parameters and, therefore, a different crystal structure formed for the Al-Mg-H mechanical alloys as compared to the Al-Mg alloys. Further analyses are needed to elucidate the differences in the mechanisms of formation of these two types of the aluminum-based mechanical alloys and such analyses are planned to be conducted as part of the anticipated Phase II research.

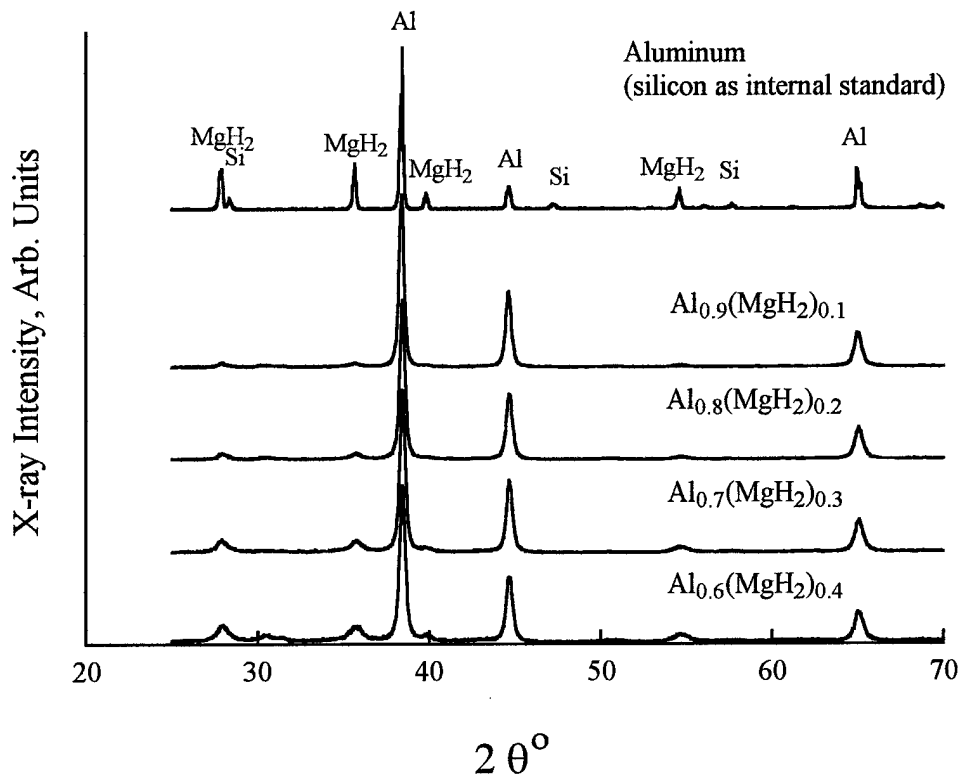


Fig. 8. X-ray patterns of the aluminum powder, and Al-Mg-H mechanical alloys

#### *Particle Sizes*

Particle size measurements for the Al-Mg-H mechanical alloys are summarized in Fig. 9 and qualitatively resemble the particle size distributions described above for the Al-Mg alloys. The mean particle sizes are quite large and the overall particle size distributions are wide. It is also observed that negligible numbers of ultrafine particles are present in the alloyed materials.

#### *Particle Morphology*

SEM images of the produced Al-MgH<sub>2</sub> alloys are shown in Fig. 10. The particle shape does not appear to change significantly with the change in composition. A large number of platelet-like particles are observed and can be found in each of the images presented in Fig. 10. The production of such particles is indicative of changes in the crystal structure occurring during mechanical alloying, although the detailed mechanism of formation of such particles is unclear and needs to be investigated in future research.

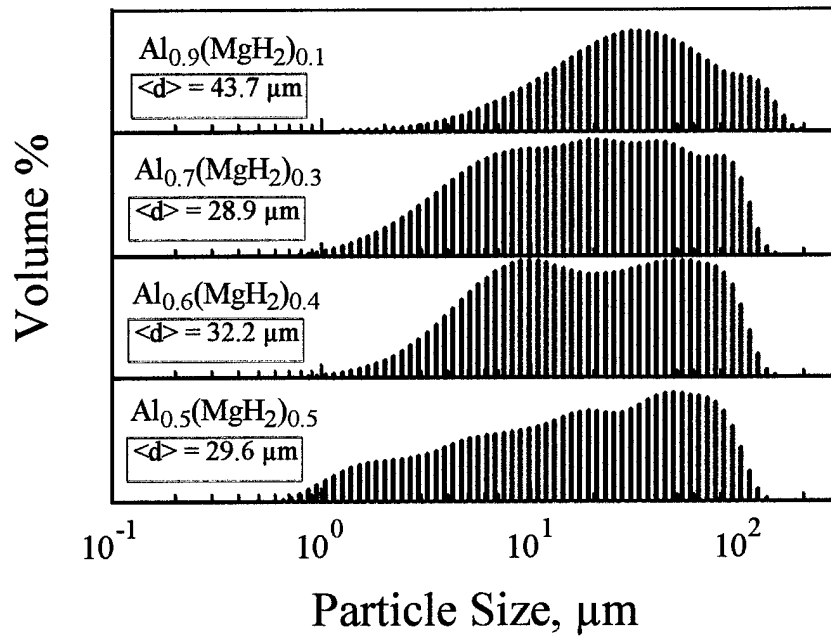


Fig. 9. Size distributions of the produced Al-Mg-H mechanical alloy powders. Mean particle sizes are labeled as  $\langle d \rangle$ .

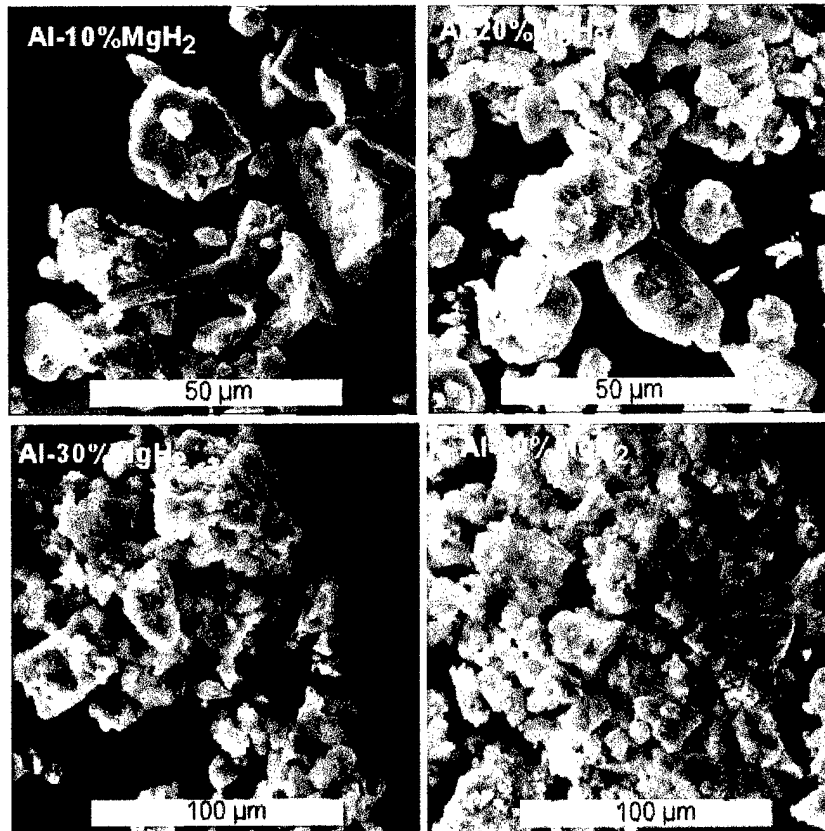


Fig. 10. SEM images of produced Al-Mg-H mechanical alloy powders

## B-Ti system

### Crystal Structure

Formation of the B-Ti mechanical alloys was expected to present a major challenge because of the anticipated reactions like  $B + Ti \rightarrow TiB$  and  $2B + Ti \rightarrow TiB_2$ . Therefore, detailed measurements of the changes in the powder structures were conducted after different ball-milling times. An example of such measurements conducted for a system containing small amounts of titanium (10 at %), is shown in Fig. 11. Because the used boron powder was amorphous, the x-ray patterns of the initial powder blend showed only pure titanium peaks. It can be seen that very soon after the ball milling started the width of titanium peaks increased significantly and their intensity decreases. At the processing time of 9 hours, the x-ray pattern shows very wide titanium peaks indicative of nano-crystalline material. The peaks are not observed to shift and therefore the titanium crystal lattice parameter was preserved. A wide and relatively weak  $TiB_2$  peak indicative of the started transformation is also observed after 9 hours.

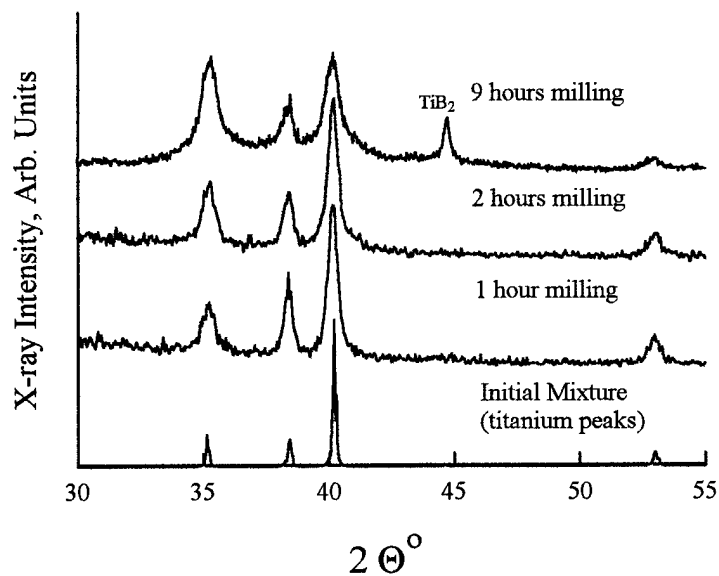


Fig. 11. X-ray patterns of the boron and titanium powder blend and a series of B- 10% Ti mechanical alloys prepared during different milling times.

The formation of  $TiB$  and  $TiB_2$  phases was observed to occur much more rapidly for B-Ti powders with 40 and 50 at % of Ti. As shown in Fig. 12, the titanium peaks observed in the initial powder blend widen quickly after only 1 hour of ball milling. It was found out that nearly complete transformation to the titanium boride phases occurred after 3 hours of ball milling, as illustrated in Fig. 12 for the powder recovered after 6-hour processing. The titanium boride powder is not reactive in oxidizing environments and therefore the alloying conditions were selected to avoid its formation. Note, however, that between 40 and 45°, at roughly the position of the strongest  $TiB$  and  $TiB_2$

peaks, a wide shoulder is observed after only 3 hours (Fig. 12). This can be interpreted as the formation of precursors of the boride phase during mechanical alloying.

It should be noted that Ti-B mechanical alloys with titanium contents of 40 and 50 at % are pyrophoric and were observed to react violently when initiated mechanically or thermally. Once ignited, such powders initially placed on a substrate as a lumped mass, self-dispersed and produced a burning aerosol cloud.

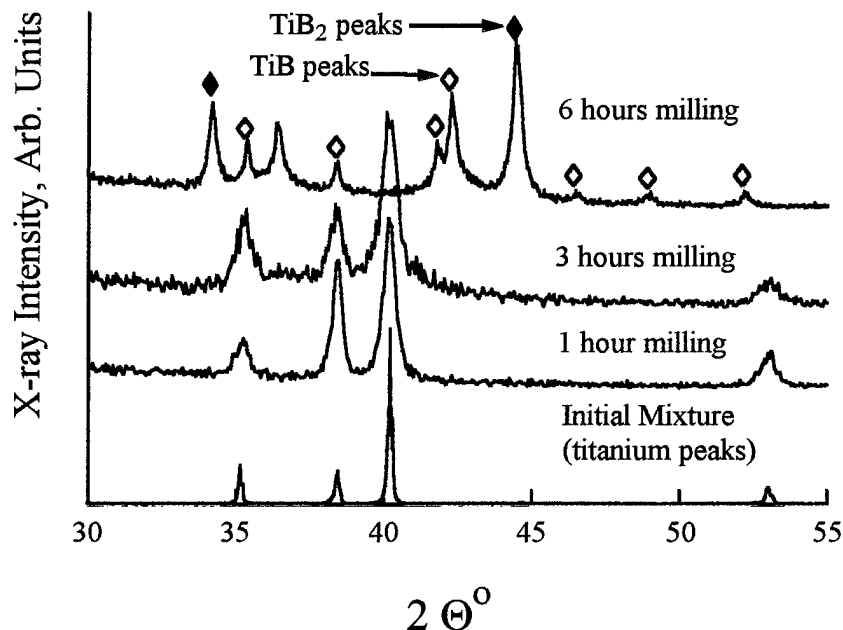


Fig. 12. X-ray patterns of the boron and titanium powder blend and a series of B- 50% Ti mechanical alloys prepared during different milling times.

#### *Particle Sizes*

Even though the initial boron powder used in preparation of mechanical alloys was extremely fine, the B-Ti mechanical alloy powders had sizes in the 10  $\mu\text{m}$  ranges as illustrated by the low angle laser diffraction measurements shown in Fig 13. Therefore, the handling procedures for such powders used in energetic formulations are expected to be much simpler than those for pure, ultrafine boron powders.

#### *Particle Morphology*

Representative examples of the SEM images showing the overview of morphology changes occurring during Ti-B mechanical alloying are shown in Fig. 14. As noted above, the size of the initial boron powder is well under 1  $\mu\text{m}$  and such fine particles are poorly resolved in the presented images. The appearance of the powders ball-milled during 1 hour is very similar to the appearance of the original titanium powder. However, the size of titanium particles initially observed to decrease and multiple surface defects (small holes) on the particle surfaces can be detected. It is likely that the holes are produced by small boron particles penetrating within titanium. With increased milling time, the particle morphology generally changes and finer particles are observed to co-exist with fairly large agglomerates. A closer look at the particle morphology reveals many interesting transient phases produced as a result of mechanical

alloying, an example of such phases is shown in Fig. 15. Long, needle-like crystals are observed to form in the B – 10% Ti alloy after 3 hours of ball milling. Based on the brightness analysis of the SEM images produced with backscattered electrons, it appears that the crystals primarily comprise of boron. These crystals are not observed in the same elemental composition samples ball-milled during longer or shorter periods. The formation of these and other structures as a result of the mechanical alloying shows that a large variety of different type intrinsic material modification processes occur and such modifications can be exploited to tailor materials properties. However, the present effort only indicates the feasibility of such material processing and a detailed study uncovering the mechanisms of the phase transformations is needed to guide an effort on engineering a broad new class of energetic materials produced using mechanical alloying.

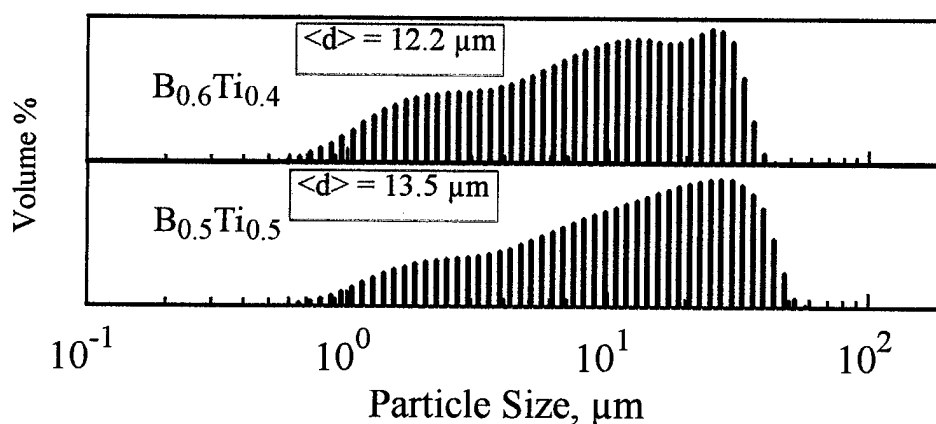


Fig. 13. Size distributions of the produced B-Ti mechanical alloy powders. Mean particle sizes are labeled as  $\langle d \rangle$ .

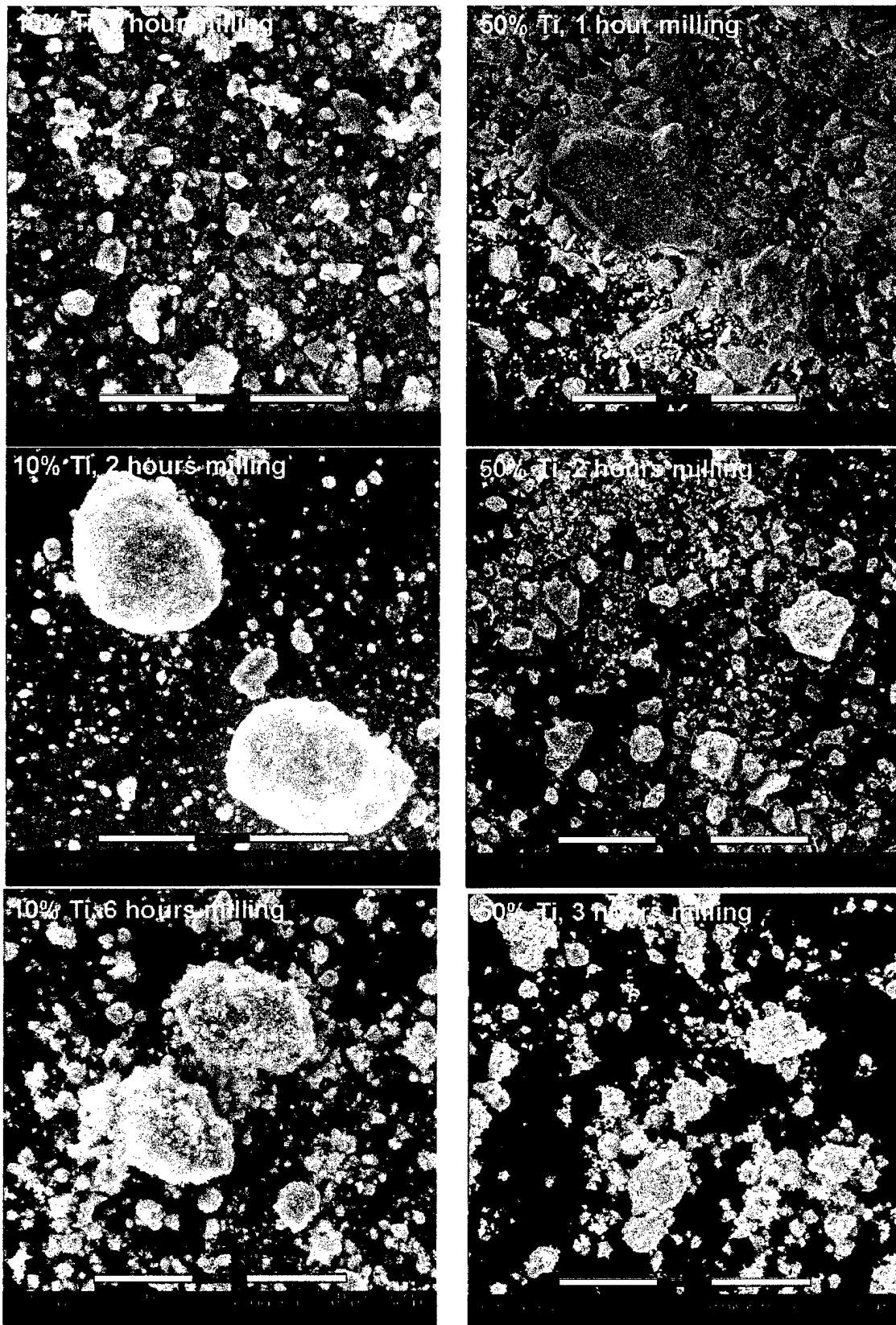


Fig. 14. SEM images of produced B-Ti mechanical alloy powders

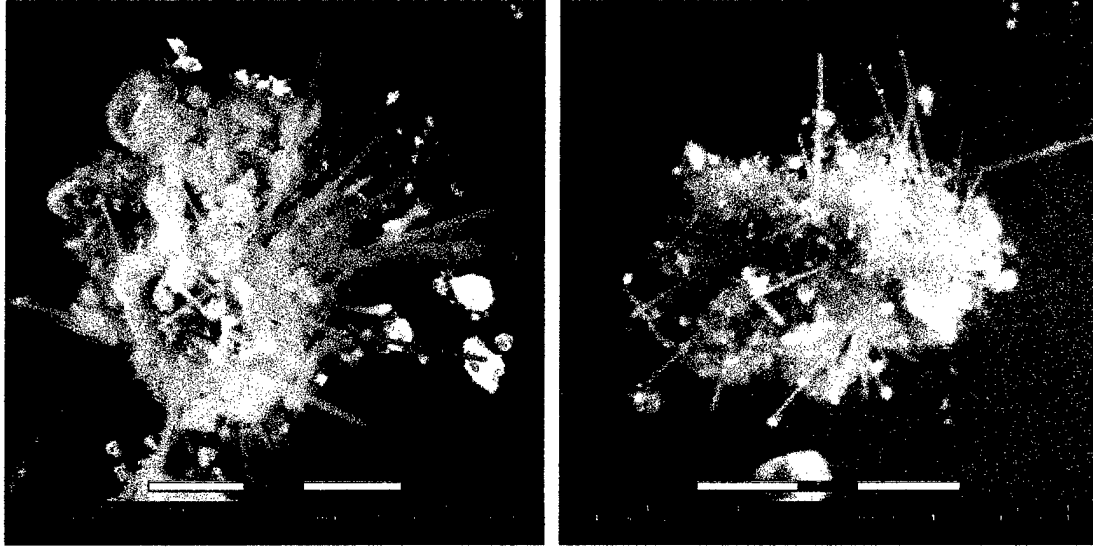


Fig. 15. SEM images showing boron needle-shaped crystals produced after 3 hours of milling of the powder mixture of boron with 10 % titanium. The image on the left produced with secondary electrons shows the particle morphology and the image on the right produced with the back-scattered electrons indicates the phase distribution: the bright inclusions are Ti.

#### Al-B and Mg-B systems

Several samples of Al-B and Mg-B mechanical alloys were prepared. The x-ray diffraction patterns for these materials are shown in Figs. 16 and 17, respectively. In both cases, the initial metal (Al and Mg) peaks appear in the powder blend in which the presence of boron powder is undetectable due to its amorphous structure. After mechanical alloying, the Al and Mg peaks broaden noticeably indicating the production of nano-crystalline phases. No boride phases were observed to form in these alloys. It is expected that a wider range of material compositions will be prepared and further characterized in the follow-up Phase II program.

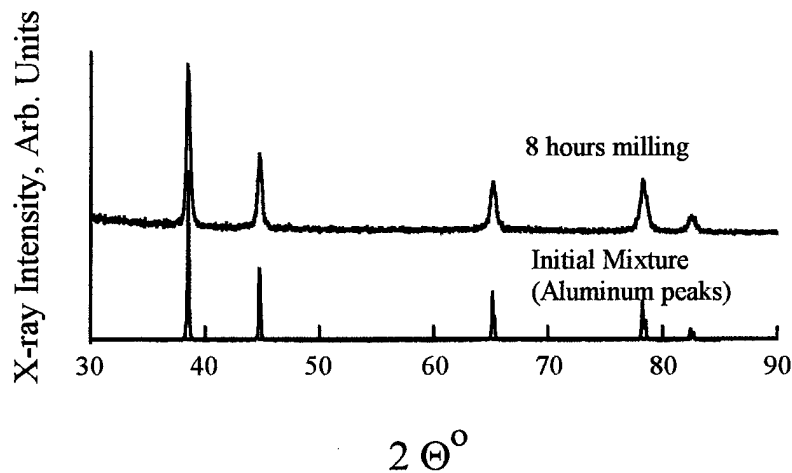


Fig. 16. X-ray patterns of the aluminum-boron powder blend and a B- 50% Al mechanical alloy.

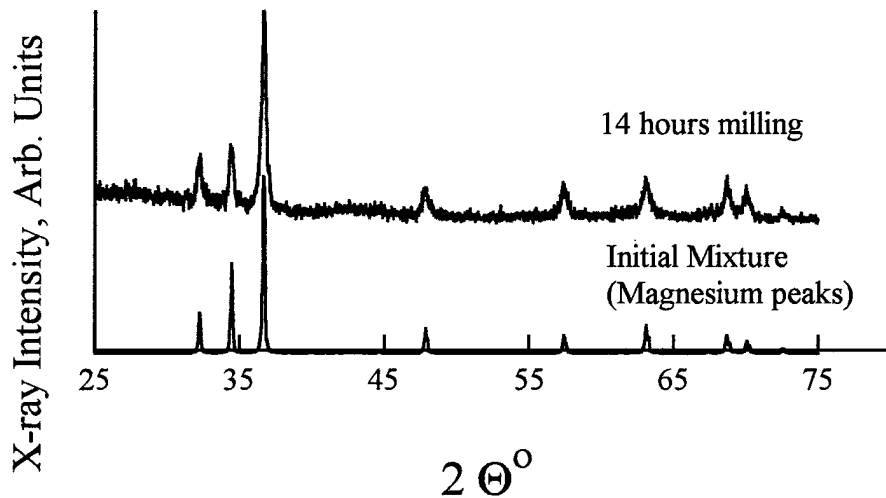


Fig. 17. X-ray patterns of the magnesium-boron powder blend and a B- 50% Mg mechanical alloy.

## VI. EXPLOSION APPARATUS AND TECHNIQUES

### A. Apparatus

The explosion apparatus used in the Phase I work was designed after the US Bureau of Mines "Hartmann apparatus" [18, 19] shown in Fig.18. The explosion chamber is constructed of two Schedule 40 type 304 stainless steel 40 cm ID welding caps. The two halves are held together by four equally spaced external clamps and sealed with an O-ring. The chamber volume is 9.2 L (7.8 and 20 L chambers have been used in explosion tests at the Bureau of Mines). A particle dispersion nozzle is positioned in the center of the bottom half of the chamber over the gas (air) inlet. The bottom half of this chamber has ports for the pressure transducer and a vacuum line. The upper half of the chamber has electrical feedthroughs for the igniter.

The explosion chamber is connected through a 15 mm ID solenoid valve to a 7.6 L air tank, which was pressurized to 470 kPa (70 psig) with commercial dry grade compressed air for dispersing the dust. The solenoid valve was used to admit a short pulse of air (0.2 s duration) to the combustion chamber, dispersing the powder through the nozzle and raising the chamber pressure to approximately 80 kPa. The solenoid valve operation and subsequent electrical initiation of the igniter was controlled by relays connected to the output of an electronic controller. In the experiments, metal powder was loaded into the dispersion nozzle, the explosion chamber sealed and evacuated, the dispersion air tank pressurized, and electronic controller tripped. The controller initiates the data acquisition system (see below), then provides 0.2 s pulses to admit the air (solenoid valve) and, after a delay of 0.3 s, provides a pulse to activate the igniter.

Hot wire igniter was made of a 5 cm long, 100  $\mu\text{m}$  diameter tungsten wires. The duration of ignition pulse was 150-180 ms, the voltage used was AC 23 V, and the current was 3.5 A. Therefore, the total energy released by the igniter was 12-15 J, much less than the energy typically used in similar experiments by the US Bureau of Mines researchers [20], typically, 400 - 500 J per igniter.

The dispersion nozzle was constructed according to the design used in the 20 L Bureau of Mines chamber [19]. The hemispherical nozzle has three rows of cylindrical holes positioned radially. It should be mentioned that in the Bureau of Mines tests a different nozzle design (the cone disperser) was also utilized. No effect of the nozzle design on the explosion tests results was reported. The sizes of the nozzle and the holes were scaled for the 9.2 L chamber using Bureau of Mines design drawing dimensions to provide the same estimated gas speed when passing through the nozzle.

A strain gauge with a range of 20 atm (2000 kPa) monitored the chamber pressure. The transducer response time is ca. 0.002 s for full-scale deflection and it has a rated accuracy of  $\pm 0.2\%$  of full scale. The transducer is housed in a 1.2 cm id pipe threaded to the chamber. The distance from the pipe end to the sensor is 1.5 cm.

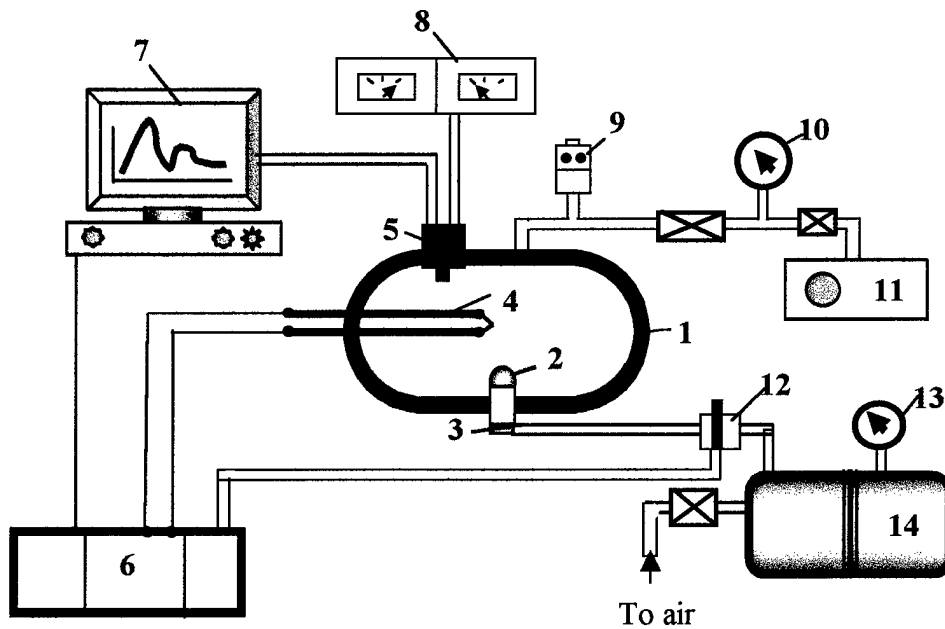
Oxygen consumption was estimated from measurements of the pressure in the chamber before and after the explosion after the temperature of the gas returned to room temperature.

The output from the pressure transducer and the time reference pulses from an electronic sequencer were stored on a PC using a RP Electronics OS-220 Scope Lab Card. Total time of the data collection in each run was 1 s. The pressure versus time curves were displayed in real time on the computer screen during the run, and the time history of the pressure transducer output (in atmospheres) saved as a file and further processed using an MS Excel spreadsheet.

## **B. Techniques**

Before each run the chamber was vacuum-cleaned and an air blast into the open chamber (top half removed) was used to clean the powder reservoir and pipes. Then a powder charge of several grams was weighed (0.01 g accuracy) and placed in the reservoir. The dispersion nozzle was then installed and an igniter wire was fixed at the center of the chamber. The chamber was closed and evacuated to 0.15-0.3 atm (in accord with Bureau of Mines procedures [18, 19]). Then the electronic controller was turned on and a triggering pulse started the data acquisition cycle. The sequence of events included an air blast, delay, and igniter initiation. During the air blast the powder from the reservoir was dispersed in the chamber and the pressure increased. The duration of the first controller pulse for the solenoid valve (dispersion pulse) was adjusted to 0.2 s to provide initial pressures,  $P_0$ , 65 - 80 kPa. Following the dispersion pulse is a short delay (0.3 s, consistent with Bureau of Mines practice) to allow the gas/particle mixture to become quiescent. According to Hertzberg [18] this time is sufficient to ensure almost stagnant gas in the combustion chamber while simultaneously minimizing the time available for particle agglomeration and gravitational settling. Then the ignitor is energized. The signal from the pressure transducer was recorded and simultaneously shown on the computer screen. After the combustion was completed and the temperature

of the explosion chamber decreased to room temperature (about 200 s), the final pressure in the chamber,  $P_f$ , was measured using the same pressure transducer.



1. Explosion Chamber
2. Dispersing Nozzle
3. Metal Powder
4. Igniter
5. Pressure Transducer
6. Controller
7. Computer for data acquisition (RP Electronics OS-220 Scope Lab)
8. Power Source (up to 30V, direct current 5A)
9. Check Valve (250 psi)
10. Vacuum Gauge
11. Vacuum Pump
12. Solenoid valve
13. High Pressure Gauge
14. Vessel with Pressurized air.

Fig. 18. Schematic diagram of the constant volume explosion apparatus

## VII. EXPLOSION EXPERIMENTS RESULTS AND DISCUSSION

The results described below cover the closed vessel explosion experiments conducted with different materials prepared in this project. Many parameters can be determined and compared as a result of such experiments, including the rate of pressure rise, ratio of the maximum to the initial explosion pressures, ignition delay time, ignition energy, flame propagation and extinction times, final pressure in the vessel after the explosion, gas composition in the vessel after explosion, condensed combustion product morphology and composition, and other parameters, such as radiation intensity. Each of these measurements is useful in elucidating the combustion mechanism, however, it should

also be noted that the interpretation of many of these measurements is not straightforward because of the complex nature of the processes occurring during explosion in a constant volume vessel. In this Phase I research, the time and funding constraints limited the types and number of the measurements conducted. The results of the measurements currently completed for different material systems are discussed below.

#### A. Mg-Al and Al-Mg-H Systems

The experimental results on explosion of Al-Mg mechanical alloys and powder blends are illustrated in Figs. 19 - 22. Figure 19 shows a series of the pressure traces measured during explosions of Al-Mg mechanical alloys and powder blends with the same elemental composition. It can be clearly seen from Fig. 19 that the alloys consistently outperform mechanical powder blends in both maximum rate of pressure rise  $dP/dt_{\max}$  (proportional to the flame speed) and maximum pressure achieved (proportional to the flame temperature). These results are significant because they confirm the hypothesis suggested in this research, specifically, that the metastable, nanocrystalline metal compounds can produce controllably higher combustion rates than the pure metals. The higher maximum pressures observed in the experiments with the mechanical alloys also indicate a more complete combustion because the overall enthalpies of reaction are essentially the same for the alloys and respective metal powder blends. The similarity of enthalpies was confirmed earlier by measurements with an oxygen bomb calorimeter [21]. Note that the absolute values of the pressures and rates of pressure rise determined in these experiments cannot be directly compared with similar values reported in earlier work using a similar experimental technique. To provide a valid comparison, the igniter energy, initial gas pressure, and the vessel shape and size must be exactly the same. However, in this work, we used ignition energies several orders of magnitude lower than that of chemical igniters used in earlier work [18 - 20]. In addition, the initial gas pressure was consistently maintained to be less than 1 atm (close to 0.8 atm) in order to limit the maximum explosion pressure while working with some of the new and highly reactive materials.

The traces of  $dP/dt$  as a function of time can be recovered from the measured pressure traces and several examples are shown in Fig. 20. Such traces can be used to analyze in detail the processes occurring in the bomb during combustion. The time when the maximum rate of pressure rise  $dP/dt_{\max}$  is observed is when the combustion wave reaches the chamber wall [22]. The continuing pressure increase (and positive  $dP/dt$  values) corresponds to the time period in which the combustion continues within the flame front. This front is quite wide for metal aerosol and very narrow for gaseous flames for which the  $dP/dt$  trace experiences a discontinuity immediately after reaching the maximum. As shown in Fig 20, the period from the time of  $dP/dt_{\max}$  to the time when  $dP/dt = 0$  (for example of a  $Al_{0.7}Mg_{0.3}$  alloy) is 22 ms. This could be interpreted as a burn time for the alloy particle of the average size for this alloy, that is 26.6  $\mu\text{m}$  (cf. Fig. 6). However, additional factors must be considered before any conclusions are drawn from such interpretations. The wide and asymmetric particle size distribution, asymmetry in the flame and the igniter position, buoyancy, and initial flow pattern present in the bomb could cause changes in the recorded pressure traces. Thus, more detailed analyses are needed that would include optical flame diagnostics and studies of the effects of the initial gas turbulence in order to analyze the details of pressure change and respective

$dP/dt$  traces. In this Phase I effort we chose to limit our analyses to comparisons of a single value of  $dP/dt_{max}$ , which characterizes the maximum achieved flame propagation rate. This value is a function of the vessel size, igniter energy, and initial conditions, all of which could be maintained constant during the project. It depends much less on the complex flame propagation processes discussed above and it is a usual practice to compare the constant volume explosion experiments based on this quantity [18 - 20].

The inconsistency in ignition delays is observed in Fig. 19, which could not be presently interpreted since several experimental issues need to be resolved first. In other words, different ignition delays could be caused by either difference in the particle size distribution or by inconsistency in the operation of the ignition circuit. Further improvements of the experimental setups are needed to address the above issues, which are considered to be suitable for the expected Phase II effort.

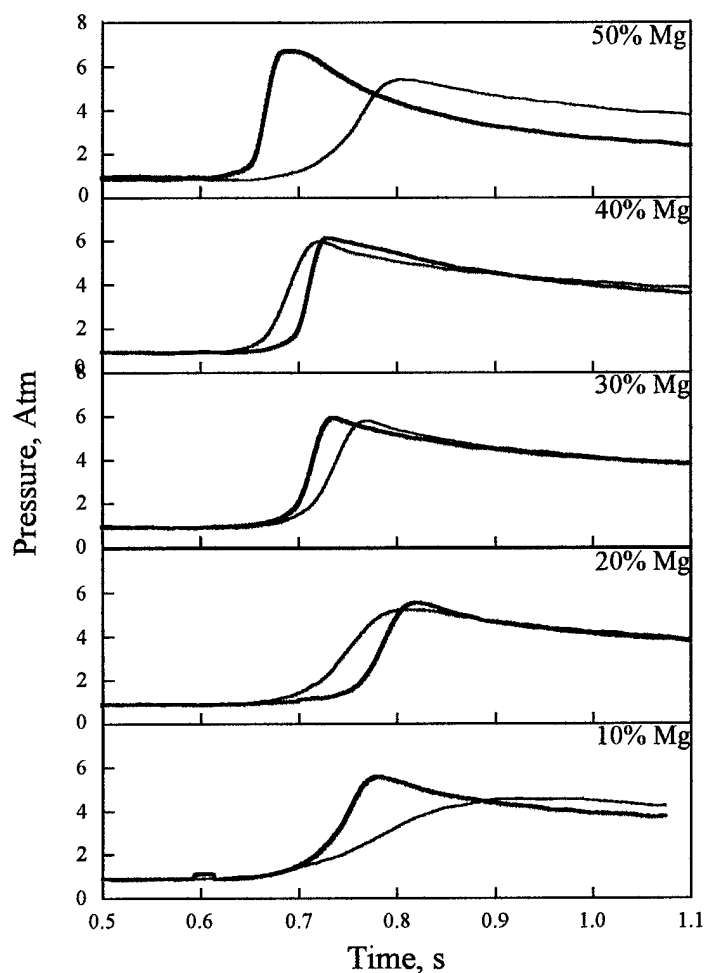


Fig. 19. Pressure traces of constant volume explosions of fuel-air mixtures with different Al-Mg powder blends (thin line) and mechanical alloys (thick line) as fuels.

A summary of the experimental results on Al-Mg and Al-Mg-H mechanical alloy systems is given in Figs. 21 and 22. The experimental results on  $dP/dt_{max}$  are compared for the prepared metastable mechanical alloys, annealed mechanical alloys that have the

same particle sizes and elemental composition, but a thermodynamically equilibrium phase composition, and Al-Mg-H mechanical alloys. The comparison shows that both Al-Mg and Al-Mg-H metastable mechanical alloys produce a higher rate of pressure rise signified by  $dP/dt_{\max}$  (and thus, a faster propagating combustion wave) than powder blends or alloys in the thermodynamically equilibrium state with the same composition. Very high rates of pressure rise are observed for the Al-Mg-H alloys with higher  $MgH_2$  contents and the differences in the combustion mechanisms of these materials as compared to the Al-Mg alloys will be addressed in future work.

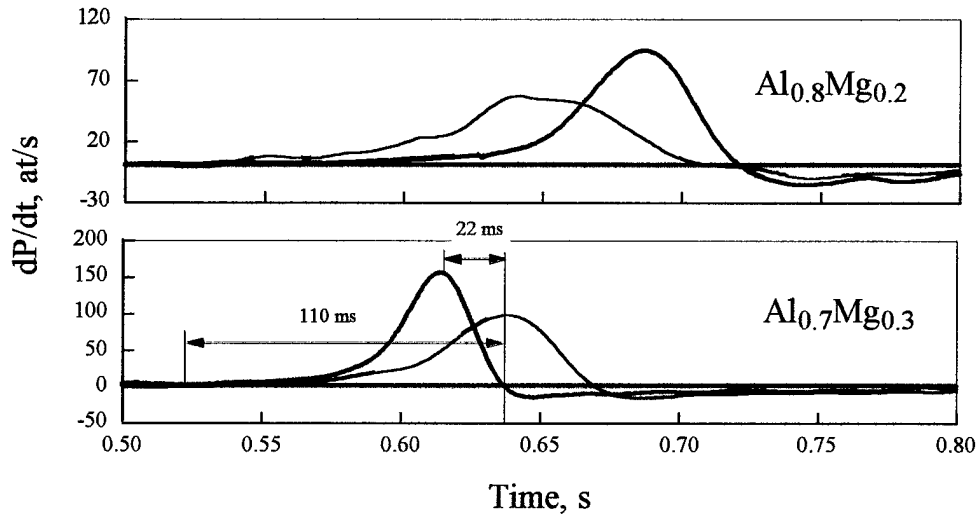


Fig. 20. Traces of  $dP/dt$  recovered from the measured pressure traces for two Al-Mg compositions. Bold lines are for mechanical alloys and thin lines are for respective powder blends.

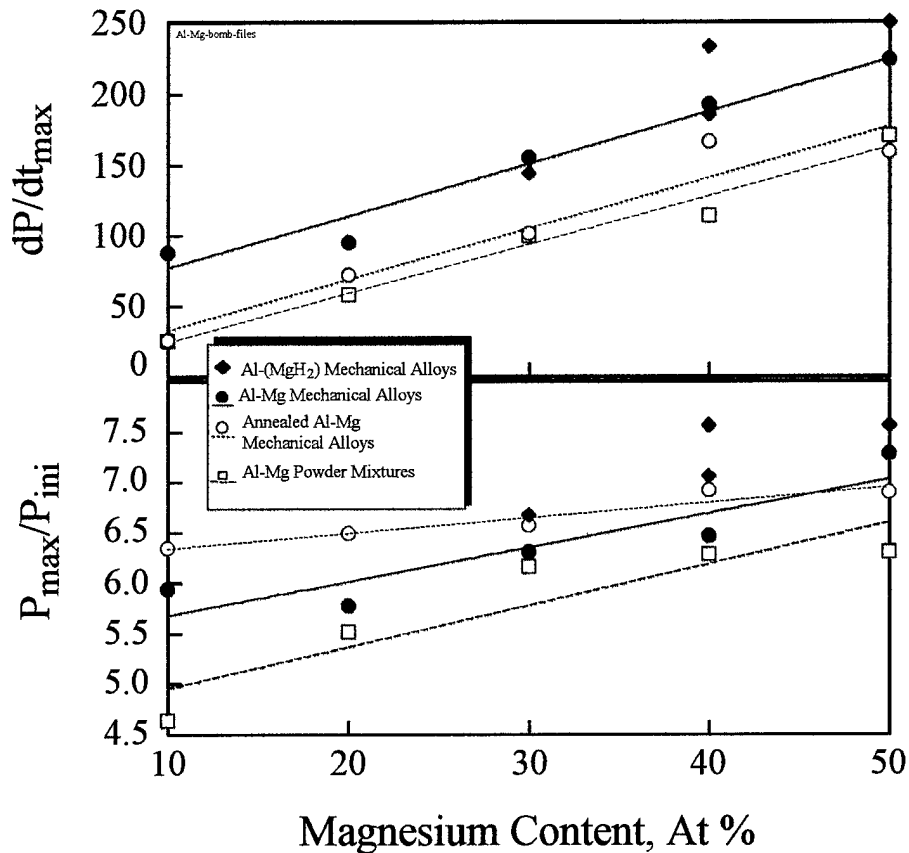


Fig. 21. Summary of  $P_{\max}/P_{\text{ini}}$  pressure ratios and maximum value of the derivative,  $dP/dt_{\max}$  for constant volume explosions of fuel-air mixtures with different Al-Mg and Al-Mg-H mechanical alloys and powder blends as fuels. Linear fits for the data sets are also shown.

Because fuel-rich mixtures with the same equivalence ratio of 1.2 were used in all experiments with Al-Mg powder blends and alloys and because the overall combustion enthalpy is essentially the same for materials with the same elemental compositions, no difference was initially expected in the measured pressure ratios  $P_{\max}/P_{\text{ini}}$ . The results obtained in this work, however, indicated some differences, e.g., somewhat higher  $P_{\max}/P_{\text{ini}}$  ratios are observed for alloys than for the same composition blends. The interpretation of this result is that a more complete reaction occurs with the alloys and this is in agreement with our analyses of the collected combustion products, as discussed below. It was also expected that the final explosion pressure would be higher in the experiments using Al-Mg-H materials and that indeed was observed as shown in Fig. 21. It is also interesting that the higher  $P_{\max}/P_{\text{ini}}$  ratios were observed for the experiments with the annealed Al-Mg alloys; however, no straightforward interpretation of this observation can be offered at this time.

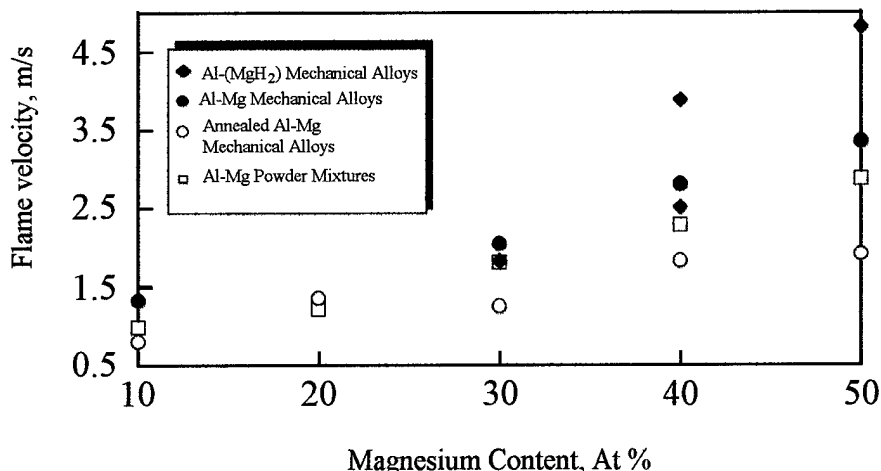


Fig. 22. Average flame velocities for the Al-Mg and Al-Mg-H systems estimated as a ratio of the explosion vessel radius to the time between ignition and the maximum observed rate of pressure rise.

The average flame velocities were also estimated as a ratio of the explosion vessel radius to the time between ignition and the maximum observed rate of pressure rise and the results of these estimates are shown in Fig. 22. The overall picture of higher velocities for nearly all mechanical alloys as compared to the powder blends and annealed powders is consistent with the higher observed rates of pressure rise. However, the average velocities estimated using the ignition time are somewhat difficult to interpret because as discussed above, these times are affected by many experimental uncertainties. The average velocities are also affected by the ignition processes during which the changes in the instantaneous flame velocity are very significant. Therefore, the interpretation of these results should be based on the detailed analyses of both ignition and combustion processes that are affected by the particle size, morphology, and composition. Unfortunately, such analyses are currently unavailable. At the same time, the comparison of the maximum rates of pressure rise (the values of  $dP/dt_{max}$ ) enables one to uncouple the ignition phenomena and compare directly the flame propagation rates. Therefore, such comparisons are currently preferred and will be made for the material systems discussed below.

Combustion products were collected after all the experiments, however, not all of the collected samples were analyzed due to the short time of this feasibility demonstration project.

Fragments of the x-ray diffraction patterns for the collected and analyzed combustion products for the Al-Mg powder blends and mechanical alloys are presented in Fig. 23.

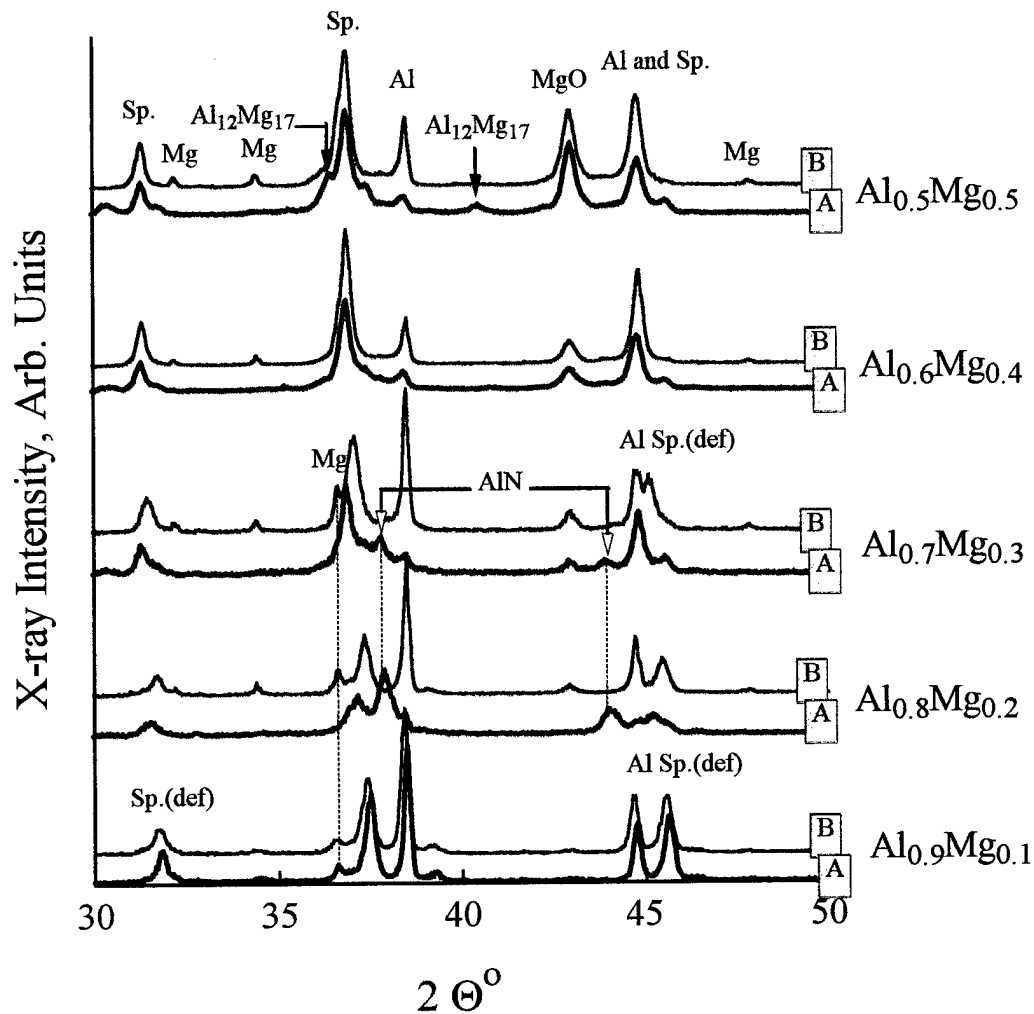


Fig. 23. X-ray diffraction patterns for combustion products of Al-Mg mechanical alloys (traces labeled with "A") and respective elemental composition powder blends (traces labeled with "B").

The analysis of the x-ray diffraction patterns have shown that spinel  $\text{Al}_2\text{MgO}_4$  (labeled as Sp. in Fig. 23) is the main product of combustion for both powder blends and mechanical alloys. The observed x-ray patterns show noticeable peak shifts, indicating that the crystal structure of the spinel phase varies with stoichiometry (Mg content) and defect concentration. The shifted spinel peaks are labeled as Sp.(def) for defect crystal structure. The x-ray patterns further show peaks of unreacted Al and Mg, most significantly in the patterns of the combustion products of powder blends. Peaks of unburned  $\text{Al}_{12}\text{Mg}_{17}$  intermetallic phase as well as weak peaks of Al are found in the products of the magnesium-rich alloys. Generally, based on the comparison of relative peak intensities it appears clear that smaller quantities of the unreacted material are present in the combustion products of mechanical alloys as compared to those of powder blends. One more interesting observation is that peaks well matching with the nitride, AlN phase are observed for the combustion products of  $\text{Al}_{0.7}\text{Mg}_{0.3}$  and  $\text{Al}_{0.8}\text{Mg}_{0.2}$  alloys whereas the peaks of unreacted aluminum nearly disappear from the x-ray patterns of

these products, but become stronger again in the products of the  $Al_{0.9}Mg_{0.1}$  combustion. As interpretation of this observation, it could be suggested that in combustion of alloys with 20 and 30 % of magnesium, sufficient amount of hot and reactive aluminum remains after the oxygen is consumed and this aluminum further reacts with nitrogen. Such a mechanism would be very interesting for many applications, e.g., it could result in significant modification of the pressure blast produced by thermo baric fuels. Further experiments and analyses are necessary to verify the proposed reaction mechanism.

It is also necessary to continue the analyses of combustion products collected in these experiments and identify the compositions of the products of combustion of the metastable Al-O-H mechanical alloys and Al-Mg equilibrium intermetallic phases.

### B. B-Mg and B-Al Systems

Only one composition (with 50 at % of boron) was prepared for each of these two materials. We were unable to ignite the prepared Al-B mechanical alloy. The experiments on ignition of the B-Mg alloy were successful and both alloy and powder blend explosion tests were conducted. The results of these experiments are illustrated in Fig. 24.

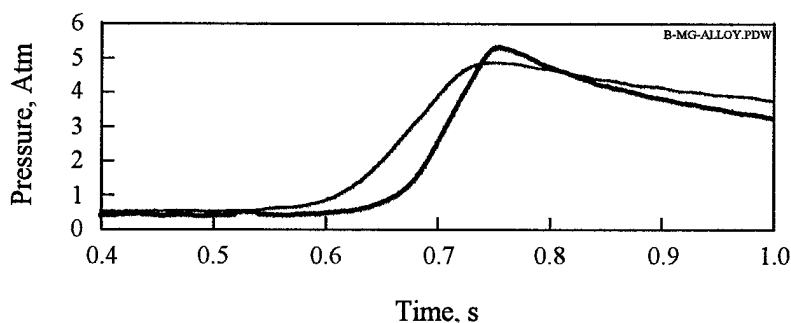


Fig. 24. Pressure traces of constant volume explosions of fuel-air mixtures with B-Mg (50 at %) powder blend (thin line) and respective mechanical alloy (thick line) as fuels.

It is observed that both maximum pressure and the rate of pressure rise are higher for the B-Mg mechanical alloy than for the same elemental composition powder blend. Therefore, the advantageous properties of mechanical alloys are qualitatively demonstrated even though further experiments and analyses are necessary for detailed description of combustion processes.

### C. B-Ti Systems

Powder blends were prepared for different elemental compositions of boron and titanium, however, the only blend ignited was with 50 at. % of titanium. At the same time, all of the prepared mechanical alloys (with 10, 20, 30, 40, and 50 at % of titanium) were successfully ignited with the same igniter energies, even though combustion of the alloy with 10 at. % of titanium was quite slow (see Fig. 25). This result already shows the improvement in ignitability of boron achieved by mechanical alloying. As noted above, the mechanical alloys with 40 and 50 at % of titanium were pyrophoric and were observed to ignite in these experiments as a result of the pressure blast rather than the

regular hot wire igniter. In other words, these two types of the alloy powders ignited before the hot wire igniter was energized, as indicated by the pressure traces shown in Fig. 25. Very fast rates of pressure rise were observed for these powders, as shown in Fig. 26. The smaller values of  $dP/dt_{max}$  and  $P_{max}/P_{mi}$  observed for the  $B_{0.5}Ti_{0.5}$  alloy are explained by the fact that the ignition occurred during the pressure blast and therefore at a significantly lower initial chamber pressure.

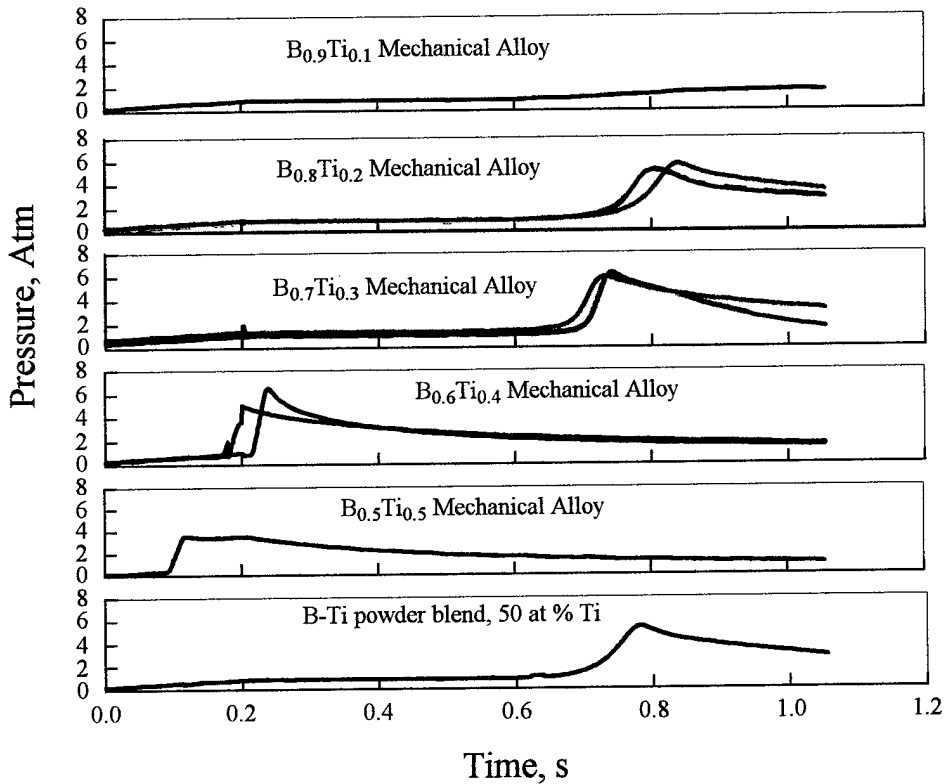


Fig. 25. Pressure traces of constant volume explosions of fuel-air mixtures with different B-Ti mechanical alloys and a 50 % Ti powder blend and as fuels. Multiple traces indicate multiple experiments with the same powders.

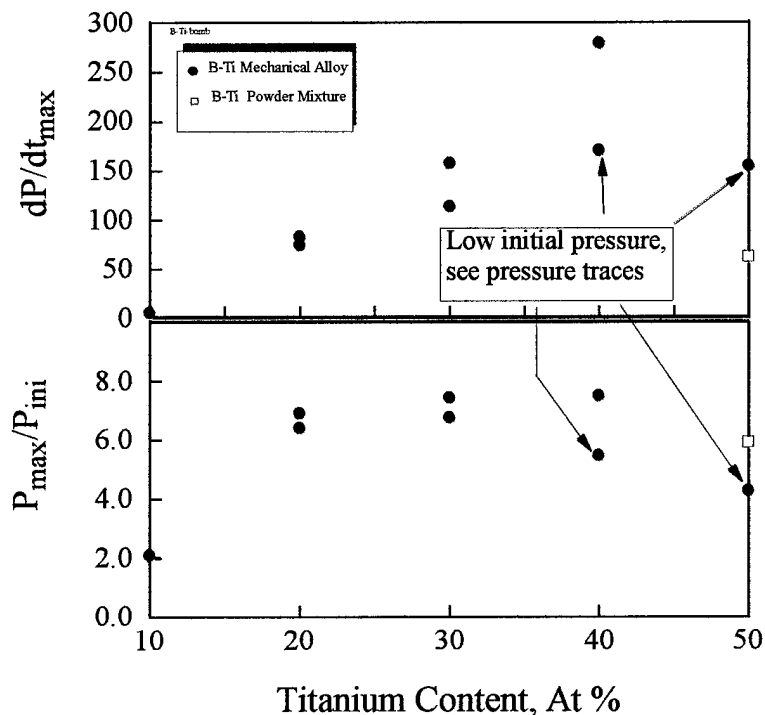


Fig. 26. Summary of  $P_{\max}/P_{\text{ini}}$  pressure ratios and maximum value of the derivative,  $dP/dt_{\max}$  for constant volume explosions of fuel-air mixtures with different B-Ti mechanical alloys and powder blends as fuels.

Combustion products of the experiments with the B-Ti powder blend (50 % Ti) and  $B_{0.5}Ti_{0.5}$  and  $B_{0.6}Ti_{0.4}$  alloys were collected and analyzed using x-ray diffraction and the results are shown in Fig. 27. The powder blend products contain significant amounts of unreacted titanium and some  $TiB_2$ , in addition to the boron and titanium oxides. It is very interesting that no appreciable titanium boride peaks are observed in the combustion products of mechanical alloys which consist essentially of a mixture of titanium and boron oxides. Therefore, the completeness of oxidation for the mechanical alloys is much greater than that for powder blend with the same elemental composition. This result seems to be significant and its interpretation will be based on the further analyses of phase changes occurring in burning mechanical alloys and powder blends. Preliminary considerations indicate that the two types of reactions, oxidation and intermetallic Ti-B reaction, occur simultaneously in the Ti-B system. Formation of Ti-B compounds is more likely to occur faster in the mechanical alloys than in the mixtures and the expected difficulty was that the formed Ti-B compounds would be less reactive with oxygen than pure metals, and thus would not oxidize completely. However, our observations indicate the opposite trend in the oxidation completeness. Also, a very fast reaction rate was observed for the alloyed materials. Therefore, it is suggested in mechanical alloys where Ti-B reactions are not limited by diffusion, these reactions occur at a very fast rate and nearly adiabatically. Thus, the newly formed Ti-B compounds are heated to very high temperatures making their complete oxidation possible. In other words, this mechanism implies that mechanical alloys enable one to significantly increase

overall combustion enthalpy in the Ti-B systems by utilizing both the intermetallic and oxidation enthalpies at the same time.

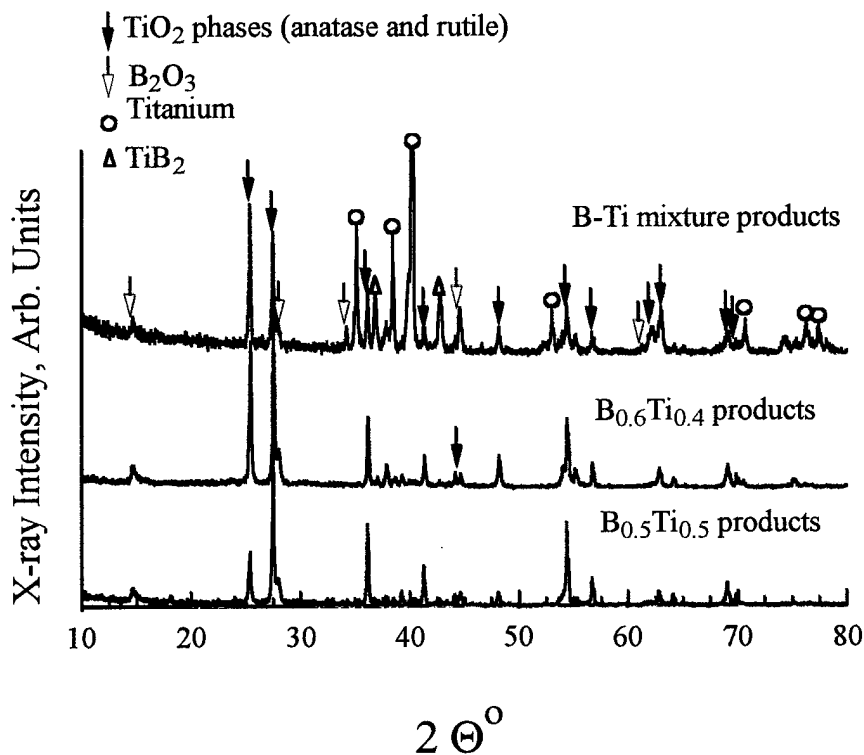


Fig. 27. X-ray diffraction patterns for combustion products of two Ti-B mechanical alloys and a power blend with 50 at % of Ti.

#### D. Aluminum powders with different size distributions

Experiments were conducted to compare explosion behavior of pure aluminum powders with different particle sizes. Two size-classified spherical aluminum powders as well as samples of commercially available aluminum nano-powders were used in these experiments. The summary of the experimental results is presented in Fig. 28 showing the measured maximum rates of pressure rise  $dP/dt_{max}$  and pressure ratios,  $P_{max}/P_{ini}$ . The results indicate somewhat higher rates of pressure rise and pressure ratios for nanosized aluminum as compared to the micron-sized particles, however, none of the measured explosion parameters comes close to those found for the mechanical alloys. Therefore, it is a conclusion of this experimental study that the prepared mechanical alloys significantly outperformed regular micron-sized as well as commercial (by Technanogy) nano-sized aluminum powders. In addition, it should be noted that the ignition of nano-sized powders was observed to occur very easily, even upon contact of particles blasted with gas with the chamber walls, however, no flame propagation was established. While it was not clear why such behavior was observed, it was found to be necessary to increase the duration of igniter heating pulse in order to achieve repeatable ignitions with the nano-sized powders. Our experience is, therefore, in agreement with many current reports, that the handling of nano-powders for energetic applications presents significant

difficulties and major research effort aimed at addressing the handling issues is needed before such nano-powders can become useful for practical applications.

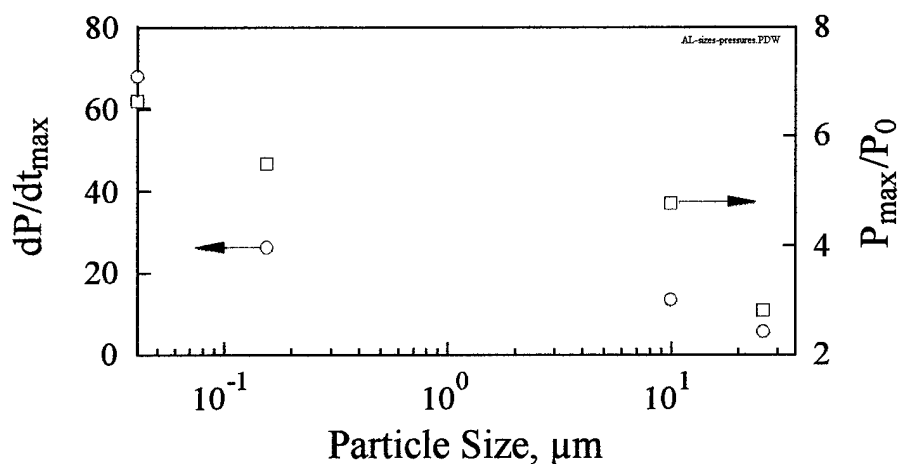


Fig. 28. Summary of the constant volume explosion tests with aluminum powders of different particle sizes. Circles show the  $dP/dt_{max}$  data and squares show the pressure ratios.

## VIII. CONCLUSIONS

The results of this work are preliminary because of its limited time and scope, however, it was affirmatively shown that different types of mechanical alloy powders could be prepared and used to improve combustion and explosion parameters of energetic formulations.

The results of the closed vessel explosion experiments in the Al-Mg material system showed that the metastable mechanical alloys exhibited higher rates of combustion and a more complete oxidation than either the reference pure powder blends of the same composition or equilibrium intermetallic phases. An additional increase in the combustion rate and pressure was achieved by using Al-Mg-H mechanical alloys. The comparison of explosion parameters and combustion products of the metastable Al-Mg mechanical alloys and pure aluminum powders of different sizes (including commercially available nano-powders) showed that much faster combustion rates, higher explosion pressures, and a more complete oxidation could be achieved with mechanical alloys. These improved combustion parameters combined with the relatively large particle sizes of mechanical alloy powders produce a combination that appears to be very attractive for practical applications: a highly energetic, readily ignitable materials that burn completely and are easy to handle and mix.

Preliminary results have shown an improvement in the boron reactivity for the prepared B-Mg mechanical alloys; however, explosions could not be initiated in the prepared samples of the Al-B alloys.

The results with the B-Ti material system are also very interesting. The feasibility of preparation of metastable and highly reactive Ti-B mechanical alloys was demonstrated. Qualitative improvements in the ignitability of boron powders

mechanically alloyed with titanium were observed as compared to the pure boron powders. The closed vessel explosion tests showed that very high combustion rates and completeness of boron and titanium oxidation could be achieved when metastable B-Ti alloys were used as fuels. It was also found that the main combustion products of the B-Ti alloys are boron and titanium oxide phases whereas significant amounts of  $TiB_2$  were observed to form in the combustion products of a blend of boron and titanium powders. Once again, it should be noted that significant improvements of the boron combustion and ignition parameters were achieved using relatively coarse mechanical alloy powders. The issue of the observed pyrophoricity of some of the produced B-Ti alloys needs to be addressed in future work.

The demonstrated ability to change the parameters of closed vessel explosions by varying the composition of mechanical alloys is regarded as an evidence of potential usefulness of such materials in novel weapon systems targeting specific underground facilities. It is also important that combustion parameter control can be achieved with metallic materials that burn more completely than pure metals and thus better exploit the high theoretical metal combustion enthalpies.

In summary, improvements in explosion rate of pressure rise and completeness of the oxidation are observed for a range of mechanical alloys and further work is needed to provide a more detailed characterization and description of the mechanical alloy combustion mechanisms and to initiate development and scale-up of the mechanical alloying powder processing for transition to practical applications.

## IX. LITERATURE REFERENCES

1. Dreizin, E.L., "Experimental Study of Stages in Aluminum Particle Combustion in Air", *Combustion and Flame*, 105:541-556 (1996)
2. Dreizin, E.L., Keil, D.G., Felder, W., and Vicenzi, E.P. "On the Mechanism of Boron Ignition" 1997 JANNAF Combustion Subcommittee, Propulsion Systems Hazards Subcommittee and Airbreathing Propulsion Subcommittee Joint Meeting, West Palm Beach, FL, 27-31 Oct. 1997
3. Molodetsky I.E., Dreizin, E.L., Vicenzi, E.P., and Law, C.K. "Phases of Titanium Combustion in Air" *Combustion and Flame*, 112:522-532 (1998)
4. Dreizin, E.L., "Experimental Study of Aluminum Particle Flame Evolution in Normal and Micro-gravity", *Combustion and Flame*, 116:323-333 (1999)
5. Molodetsky, I.E., Dreizin, E.L., and Law, C.K. "Evolution of Particle Temperature and Internal Composition for Zirconium Burning in Air" *Twenty-Sixth Symposium (Int'l) on Combustion*, The Combustion Institute, Pittsburgh, 1997, pp. 1919-1927
6. Dreizin, E.L., "On the Mechanism of Asymmetric Aluminum Particle Combustion", *Combustion and Flame* 117:841-850 (1999)
7. Dreizin, E.L., Keil, D.G., Felder, W., and Vicenzi, E.P., "Phase Changes in Boron Ignition and Combustion", *Combustion and Flame* 119:272-290 (1999)
8. Dreizin, E.L., "Phase Changes in Metal Combustion" *Progress in Energy and Combustion Science*, 26 (1):57-78 (2000)

9. Shoshin, Y.L., Mudryy, R., and Dreizin, E.L., Preparation of Al-Mg mechanical alloys and testing their ignition and combustion parameters. *2<sup>nd</sup> Joint Meeting of the US Sections of the Combustion Institute*, Oakland, CA, 2001 (submitted)
10. Benjamin, J.S., *Metal Powder Rept.*, 45:122 (1990)
11. Suryanarayana, C (Editor) *Non-equilibrium processing of materials* Amsterdam ; Oxford : Pergamon, 1999
12. Wen, C.E., Kobayashi, K., Sugiyama, A., Nishio, T., and Matsumoto, A., *Journal of Materials Science* 35:2099 – 2105 (2000)
13. Nebti, S., Hamana, D., and Cizeron, G., *Acta metall. Mater.* Vol. 43, No. 9., pp. 3583 – 3588 (1995)
14. Lu, L., Zhang, Y.F., *Journal of Alloys and Compounds* 290:279 – 283 (1999)
15. Clark, C.R., Suryanarayana, C., and Froes, F.H., *Synthesis/Processing of Lightweight Metallic Materials* (Froes, F.H., Suryanarayana, C., and Ward-Close, C.M., Editors) The Minerals, Metals & Materials Society, 1995
16. Massalski, T.B., Okamoto, H., Subramanian, P.R., and Kacprzak, L. (Eds) *Binary Alloy Phase Diagrams*. ASM Publ., Materials Park, OH, 1990
17. Suryanarayana C. Mechanical Alloying and Milling *Progress in Materials Science*, 46 (2001) 1-184.
18. Hertzberg, M. Cashdollar, K.L., and Opferman, J.J., "The Flammability of Coal Dust-Air Mixtures," US Bur. Mines RI8360 (1979)
19. Cashdollar, K.L. and Hertzberg, M., "20-l Explosibility Test Chamber for Dusts and Gases," *Rev. Sci. Instrum.* 56, 596. (1985)
20. Cashdollar, K.L. and Chatrathi, K., "Minimum Explosible Dust Concentrations Measured in 20-L and 1-m<sup>3</sup> Chambers," *Combust. Sci. Technol.* 87, p. 157 (1992)
21. Dreizin, E., Shoshin Y., and Mudryy R., "High Energy Density Powders Of The Al-Mg Mechanical Alloys", 50th JANNAF Joint Propulsion Meeting, Salt Lake City, UT, July 11-13, 2001
22. Lewis, B., von Elbe, G. *Combustion, Flames and Explosions of Gases*. Academic Press, New York, 1987.